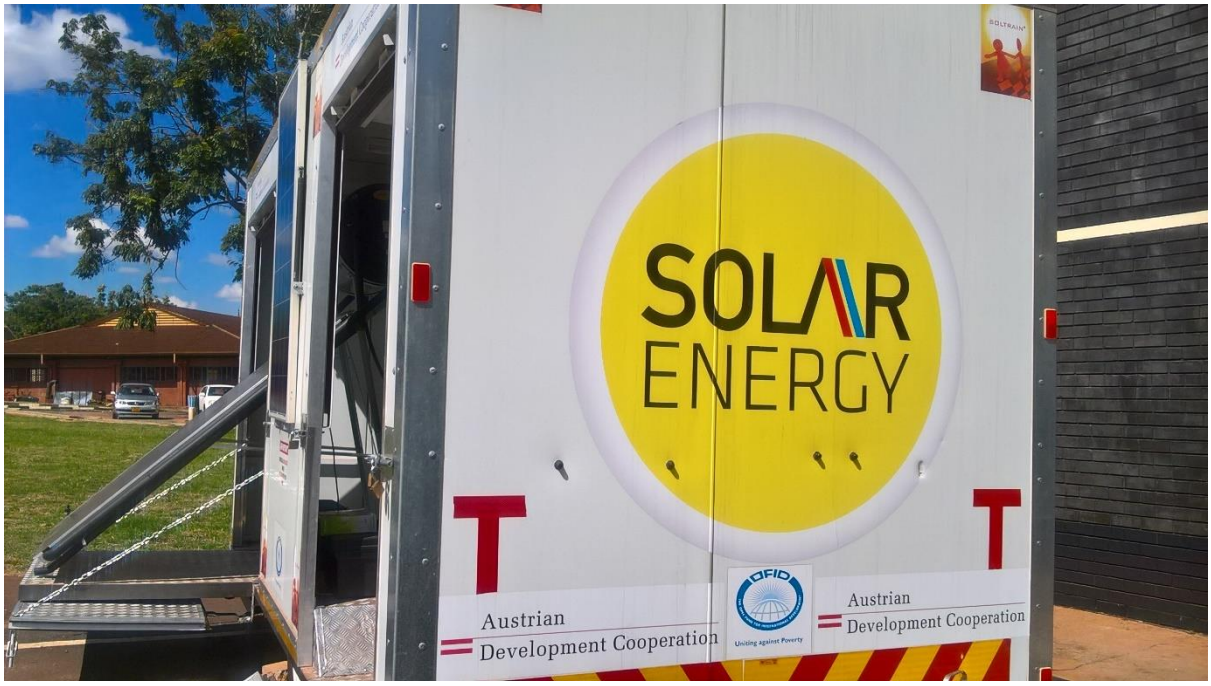
SOLAR
ENERGY
Austrian
Development Cooperation
OFID
Austrian
Development Cooperation


CONTROL BOARD

DISSERTATION TITLE: A simple method of characterising solar thermal water heating systems (SWHS) and the prediction of thermal and economic performance of the SWHS.

By

Wilson Rutsate

Supervised by

Eng. Tawanda Hove

In partial fulfilment of the requirements of the Master of Science degree in Renewable Energy Engineering.

Department of Mechanical Engineering

University of Zimbabwe

September 2017

DECLARATION

May it be known that the results of this research were the sole efforts of Wilson Rutsate and the quoted references? I assume responsibility for any errors that remain.

Signed…….....

Date……..

ABSTRACT

This research is based on manipulating the Hottel-Whillier-Bliss equation to determine the performance characteristics $F_R\bar{\tau}\alpha$, F_RU_L and Us of the system by substituting mass flow $\dot{m}$ in the collector based equation ;
$\dot{m}cp\Delta Ts = A_cF_RG_T(\bar{\tau}\alpha)_n - F_RU_L(Ti-Ta)$ with
$\frac{dT}{dt}$ in the collector- storage tank system equation;

$Mcp\frac{dTs}{dt} = A_cF_RG_t(\bar{\tau}\alpha)_n - (A_cF_RU_L+U_sA_s)(Ts-Ta)$.
This is an innovative and cost effect approach to achieve results that would otherwise require sophisticated equipment and gadgetry.

Measurements of radiation, G_t and temperatures, Ts and Ta were taken and the optical and thermal parameters to construct a performance model were evaluated. The resultant model was tested on clear days by measuring actual storage tank temperatures and compared them with the predicted ones.

The results showed that this novel method can be used to characterise solar water heating systems to get satisfactory if not excellent results. This information was further used to predict the performance of load simulated SWHS in Harare in any month of the year given meteorological information that is readily available.

ACKNOWLEDGEMENTS

I wish to thank all those who made the research possible and helped me during the course of my study. First and foremost my utmost gratitude go to my supervisor Engineer Tawanda Hove, whose guidance, incisive and constructive criticism based on a fountain of knowledge bone out of passion for the subject, gave this work the face that it has assumed.

My thanks go to other members of staff for the renewable energy course, Engineers L Madiye, C S Shonhiwa, Mr Munjeri, Prof Chikuni, Prof Mashonjowa, Prof Gutu, Dr Musara, Dr Kutsodza. All their courses helped form a solid theoretical foundation to enable one to navigate comfortably through the task of writing a renewable energy dissertation.

I would like to express my gratitude to the engineering staff at the faculty who helped me with logistical support for the Solar Trailer; Mr Raymond Chikotosa from the mechanical engineering department and Mr…… from the electrical engineering department.

My acknowledgement to my wife Liz for her support and encouragement. The kids for their understanding when at times I had to come late in the night or early morning collecting data.

Last but not least the MRE group who made studying for this course an enjoyable and yet rewarding experience.

LIST OF TABLES

LIST OF FIGURES

LIST OF ABREVIATIONS

SWHS……solar water heating systems

SRCC…….solar rating and certification corporation

DTC……differential temperature controller

FPC …….flat plate collector

CHWT…….compact hot water tank

DHWT…….domestic hot water tank

DHWD……daily hot water demand

kWh……kilo watt hours

MJ/m^2 ……Mega Joules per square metre

W/m^2……Watts per square metre

˚C …….degrees centigrade

IEA …….International Energy Agency

SF……Solar Fraction

NOMENCLATURE

δ	Declination angle
θ	angle of incidence
θ_z	zenith angle
Φ	latitude of the location in question
Υ	collector axis relative to the North-South axis
Υ_S	solar azimuth position of the sun relative to the North-South axis
ω	hour angle – position of the sun relative to the axis of the local meridian
β	angle of tilt of the collector to the horizontal
T_i	inlet fluid temperature to the collector
T_{st}	tank storage temperature
T_a	ambient temperature
G	global radiation on the horizontal plane
G_{sc}	solar constant
G_T	global radiation on the tilted plane
n	day number
I_O	hourly extra-terrestrial radiation on a horizontal plane
I_d	hourly diffuse radiation on a horizontal surface
I_T	total hourly radiation on a tilted plane
k_T	hourly clearness index
k_θ	incidence angle modifier
H_o	monthly average daily extra-terrestrial radiation on horizontal plane
$\bar{H}$	monthly average daily radiation on a horizontal plane
F_R	heat removal factor
L_{st}	standard meridian for the local time zone

L_{loc} longitude of the location in question

E equation of time

ΔT_S increase or decrease in storage temperature

U_L collector overall heat loss coefficient

A_C collector aperture area

U_S heat loss coefficient of storage tank

As surface area of storage tank

ʈ collector cover transmittance factor

α collector absorber absorbance factor

η collector efficiency

Q_i incident radiation on the collector

Q_U useful heat gain

Q_O heat loss

t time in seconds

M mass of water in the storage tank

Cp specific heat capacity of water

CHAPTER I

1.1 INTRODUCTION

In Zimbabwe solar water heaters have been positively received by home owners and authorities alike. This is mainly due to their real value in saving electrical energy from the grid when there is sufficient insolation to provide solar heating. The other reason for this apparent popularity is the simplicity of the system. It is very easy to install and maintenance is minimal. The low temperature ranges to which they belong, suits the domestic requirements of temperatures below 100˚C very well. As a result many solar water heating systems (SWHS) have been brought into the country without having been subjected to a rigorous solar rating and certification criteria SRCC OG-300 which deals with solar water heating systems certification or SRCC OG-100 which deals with collector certification. (SRCC, 2006)

The performance of these solar water heating systems is therefore largely unknown and left to claims of their distributers and their sometimes overzealous sales persons who oftentimes make unrealistic performance claims owing to their otherwise lack of the requisite knowledge and understanding of the parameters involved.

Being a relatively new technology the monitoring and regulatory authorities are overwhelmed by the influx of these new products and do not have the requisite frame work to handle the testing and certification criteria. It is against this background that this project seeks to provide a simple characterisation method of solar water heating systems. Thus the project will provide a starting point for control, monitoring, testing and eventually certification of SWHS.

Research has shown that solar water heating is indeed an economically viable option in Zimbabwe. Kagande et al (2013)

provided a technical and economic justification for solar water heating system as a viable option in this country. In the National Energy Policy for Zimbabwe, in 7.5.5.5, the Minister adds more impetus to the use of solar water heating systems referred to in the policy document as solar geysers. Some of the measures proposed seek to make it mandatory for new houses to be equipped with solar geysers accompanied by various penalties to be imposed for non-compliance. National Energy Policy (2012)

It is also important to disabuse the notion held by ordinary people that solar water heaters can replace electric geysers by the simple act of their installation. To add salt to injury the media quotes unrealistic power savings by the simple act of installing a specified number of solar water heaters. It is important to understand the concept of solar fraction which is the ratio of the energy provided by solar energy to the total energy demanded for a particular energy requirement e.g. water heating in this case. There is therefore a need to distinguish between energy saving and power saving. Energy saving is basically power saved by provision of heat by solar water heaters outside the peak period. Power saving is the energy saved during the peak period when the solar device is supplying energy and thus relieves the strain on the power utility.

Solar water heaters especially for domestic usage have a demand profile peaking normally in the mornings and evenings when usage is at its maximum. Meyer (2000) It is only under these demand conditions that hot water from solar geysers will make an impact on grid savings and the likelihood of impacting on grid capacity not just energy savings. Unfortunately from the intermittent nature of insolation it is not possible to completely match demand and heat energy production from the sun and therefore make a huge impact on grid savings.

1.2 Background

In Zimbabwe solar water heating is a relatively new technology and therefore not readily understood by the common people. Knowledge and understanding of the terms is largely rudimentary. The methods of testing performance parameters are fairly complicated requiring sophisticated and expensive gadgetry. This is done in specialist laboratories where environmental parameters are simulated.

Theoretically the parameters can be evaluated by applying concepts of radiation physics and thermal physics. All these might not excite people outside the academic circles. Field test basically bridge this gap where experimental evaluation of performance parameters though not ignoring radiation physics, thermal physics and fluid dynamics tends to be more intelligible to practically oriented people with less drive for theoretical physics.

1.3 Problem statement

Solar water heating systems that are installed in people's houses are configured as collector - storage tank systems and for testing purposes it is not possible to isolate the individual units. The gadgetry is such that there is no provision for measuring collector inlet fluid temperature and there are no flowmeters to measure the heat transfer fluid flow. This is the most common configuration of SWHS found in Zimbabwe.

Regulatory authorities need a simple method of characterising SWHS in an outdoor environment that is typical of the operating conditions of the installed gadgets. Consumers need to know the performance of these gadgets before purchase so that they can make an informed decision about purchase.

1.4 Justification

The justification of this research is that a simple cost effective method is proposed against a complicated method complete with expensive equipment and gadgetry. The theoretical framework is sound based on an understanding of thermal physics, radiation physics, fluid dynamics, some thermodynamics and the behaviour solar thermal collectors and storage tank systems at a fairly advanced level.

1.5 Research Questions

What is this research seeking to achieve?

Who are the beneficiaries of this study?

Is this research going to add to knowledge value and better understanding of the subject?

Does this study have any relevance to the community?

What does it cost to implement this research?

1.6 Aims and Objectives

The aim of this study is to provide answers to the above research questions and be able to characterise the performance of SWHS completely using a simple methods utilising only the very basic gadgetry that is required to determine required parameters.

The objectives are:

- To determine the optical parameters of the SWHS; $F_R(\tau\alpha)_n$
- To determine the overall thermal loss coefficient of the system ($F_R U_L + \frac{UsAs}{Ac}$) by studying the combined system.

- To determine the storage tank loss coefficient $UsAs$ by studying the tank separately under conditions of zero irradiation and then infer the heat loss coefficient F_RUs for the collector.
- To be able to predict and validate the thermal performance of the system under different conditions.
- To be able to evaluate the solar fraction of the system.
- To be able to evaluate these parameters throughout the year.
- To be able to make an economic evaluation of the system.

1.7 Summary of methodology.

The study was conducted on the solar trailer which is a training solar unit (Fig. 1 and Fig.2) donated by the Austrian Development Agency to the University of Zimbabwe. The study was limited to the thermosiphon system which does not have flowmeters.

Readings of storage tank temperatures, ambient temperatures, and horizontal radiation at the solar trailer as well as any changes in radiation income influenced by shading were captured. The readings were taken every 15 minutes from 8 o'clock to mid night.

The radiation on the horizontal surface was transformed to correspond to the radiation on a tilted plane using the relevant sky models. Tables resulting in the construction of the Hotell- Whillier-Bliss equation which makes use of the theories developed mostly from radiation physics and thermal physics.

This data captured during daytime enabled the evaluation of the above equation by a regression method in excel to evaluate F_RƮα as well as ($F_R U_L + \frac{UsAs}{Ac}$). The data capture outside daytime was used to generate the temperature decay information to evaluate the storage tank heat loss coefficient. It then becomes possible to isolate

mathematically the two loss coefficients relating to the collector and the storage tank.

Having generated the performance data a mathematical model was constructed and clear days were chosen to measure tank temperatures during day and during night and compare with the predicted temperatures from the model. This is the simplest way of validating the model.

After validating the model it was now possible to answer the objectives stated above making use of this powerful mathematical model.

1.8 Assumptions and Limitations.

- The basic assumptions are that the fluid medium is at saturated vapour state.
- The instrumentation is well calibrated.
- Second order effects and terms are insignificant.
- The temperature profile in the storage tank is homogeneous and not stratified.
- Pipes losses assumed at 10%
- The effect of wind is speed less than 2m/s is negligible
- The heat removal factor F_R and the heat heat loss coefficients U_L and U_S are constant.
- The model assumes that the storage temperature is what the collector “sees” as the inlet temperature. This is not absolutely correct as only the stratified lower temperature water of the tank is siphoned into the collector.

The limitations arise from:

- The time of measuring the parameters was not really instantaneous but influenced by the human factor. A data logger could have assisted a great deal.

- The radiation on a tilted surface was not measured directly but had to be inferred from sky models.
- There are always some intrinsic errors from measuring instruments.
- In between the 15 minutes intervals a lot happens in the dynamic sky cloud system. As a result on some days attempts at taking measurements were aborted as the sky clouds were playing havoc in between readings rendering the data meaningless?

Who will benefit from this research and how?

Test methods for determining the thermal performance of solar water heating systems are intended to provide objective information that can help local manufacturers to design SWHS that will perform under a range of meteorological conditions. The same tests can help consumers to compare the performance and cost effectiveness of competing products. Monitoring authorities can tap from this research to put in place testing and monitoring protocols to approve and disapprove products that meet or do not meet the minimum criteria for the line of products. Learning institutions can further develop the methodologies developed in this research and help in the customisation of testing methods for Zimbabwean conditions.

CHAPTER 2

Literature Review

This literature review deals with the basic concepts of solar radiation, solar water heaters, flat plate collectors and thermal storage systems. This will acquaint the reader with the basic terminology, concepts and formulae upon which this research is based. These formulae will be explained in sufficient detail so as not to overwhelm the reader who might not be a renewable energy specialist. The basic text books by John A. Duffie and William A. Beckman (2013) Solar Engineering of Thermal Processes as by Soteris A. Kalogirou (2009) can assist the reader who has developed a special interest in solar thermal collectors and would like to get more insight. Equations 2.1 to 2.35 are extracted from Duffie J.A. (2013) while equations 2.36 to 2.39 are extracted from Kalogirou (2009).

2.1 Solar Radiation

Most renewable energy available can be traced back to the sun as its origin. Solar energy is used directly in PV panels to convert it to electricity and in solar collectors to convert it to heat for hot water or for air conditioning. Wind energy can is derived from differential heating of the earth's crust leading to temperature gradients that generate wind. The wind and the sun's heat cause water from the water bodies to evaporate causing water vapour and rain or snow which flow downhill into rivers and this energy is captured using hydropower schemes. Biomass itself is derived from sunlight as

plants grow extracting carbon dioxide from the atmosphere during the photosynthetic process.

Scientifically the sun's surface can be modelled as a black body. At the surface temperature of 5777˚K this black body emits energy with a unique radiation spectrum covering the ultraviolet range from 0 - 0.38µm, the visible range from 0.38µm – 0.78µm and the infrared range from 0.78µm – 1mm.

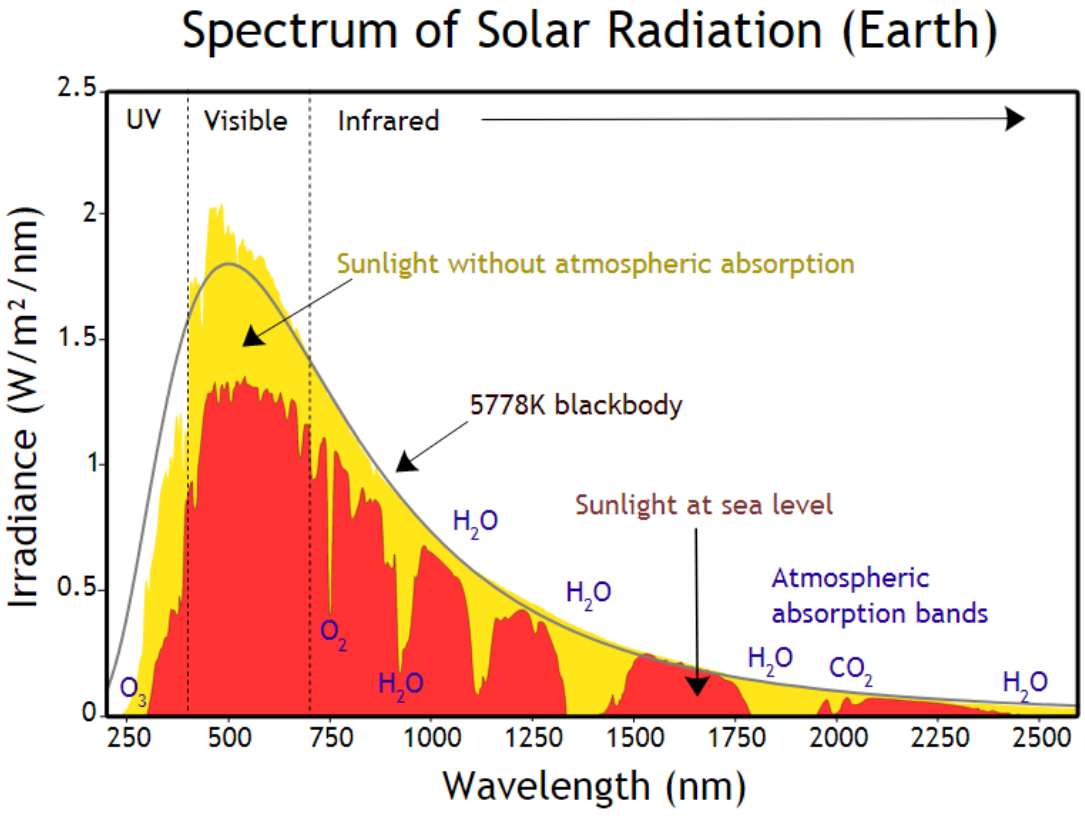

Fig 2.1 Spectral distribution of extraterrestial radiation

Source: https://en.wikipedia.org/wiki/Sunlight#/media/File:Solar_spectrum_en.svg

2.1.1 Extra-terrestrial Solar radiation

The amount of solar energy per unit time, at the mean distance of the earth from the sun received on unit area of a surface normal to the direction of beam radiation outside the earth's atmosphere is called the solar constant G_{sc}. When the sun is closest to the earth on January 3, the solar radiation at the outer edge of the earth's atmosphere is about 1400 W/m^2 and when furthest away on July 4 it is about 1330 W/m^2. When it is at the mean distance it is 1367 W/m^2.

Fig 2.2

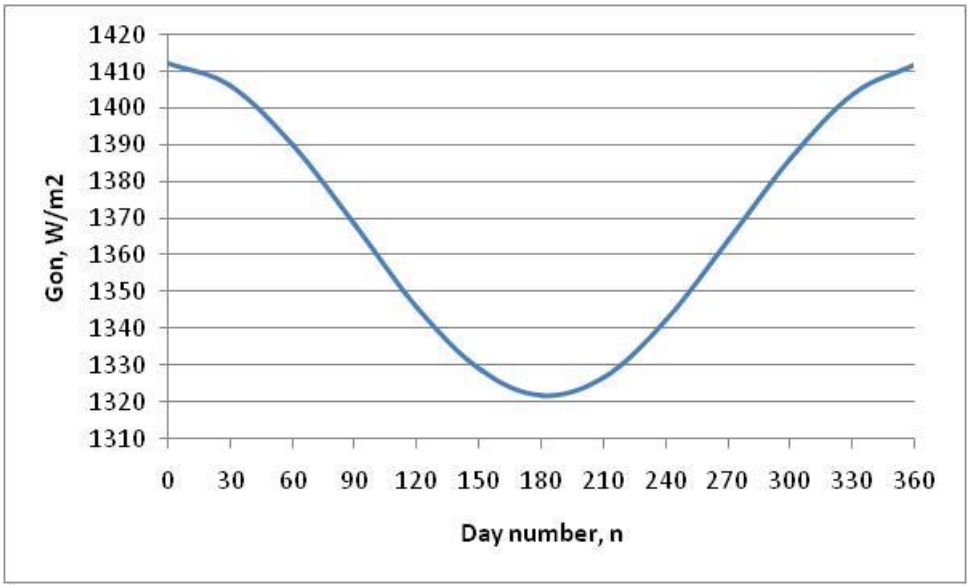

Variation of terrestrial radiation with day number of the year.

The global radiation on a horizontal surface is given by:

$$G_o = G_{sc}\left[1+0.033\cos\left(\frac{360N}{365}\right)\right]\cos\Theta_z \qquad (2.1)$$

Solar declination Angle δ

The plane of the earth's revolution around the sun is called the elliptic plane. The Earth itself rotates around an axis called the polar axis which is inclined at approximately 23.45˚ from the normal to the elliptic plane. The earth's rotation around its axis results in day and night while the position of the axis relative to sun causes seasonal changes in solar radiation income.

The angle between the polar axis and the normal to the elliptical plane remains unchanged at 23.45˚ that is to say the angle between the earth's equatorial plane and the elliptical plane is constant. However the angle between the line joining the centres of the sun and the earth to the equatorial plane changes all the time. This angle is the declination angle and is defined thus:

$$\delta = 23.45\sin\left(360\frac{284+n}{365}\right) \qquad (2.2)$$

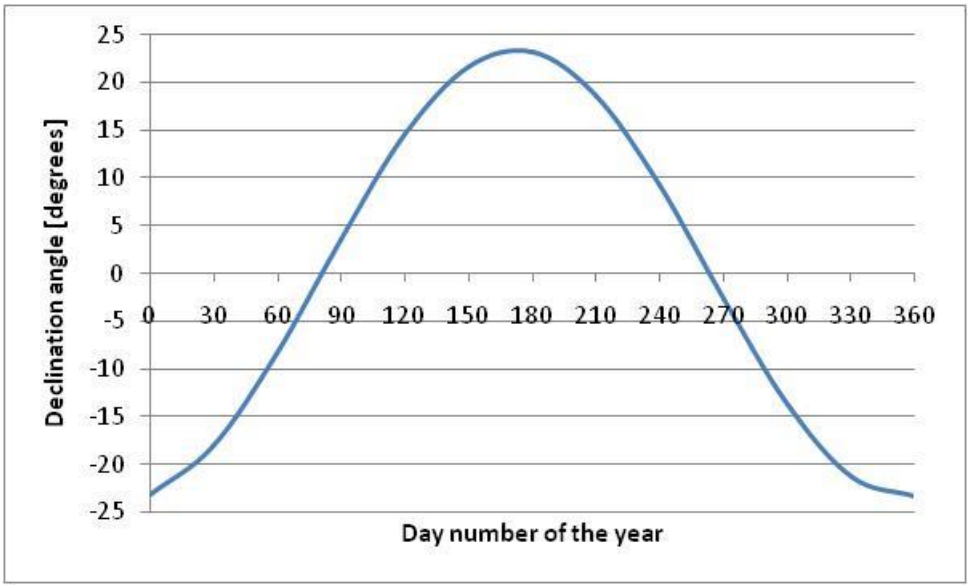

Fig.2.3 Variation of declination angle with day number of the year.

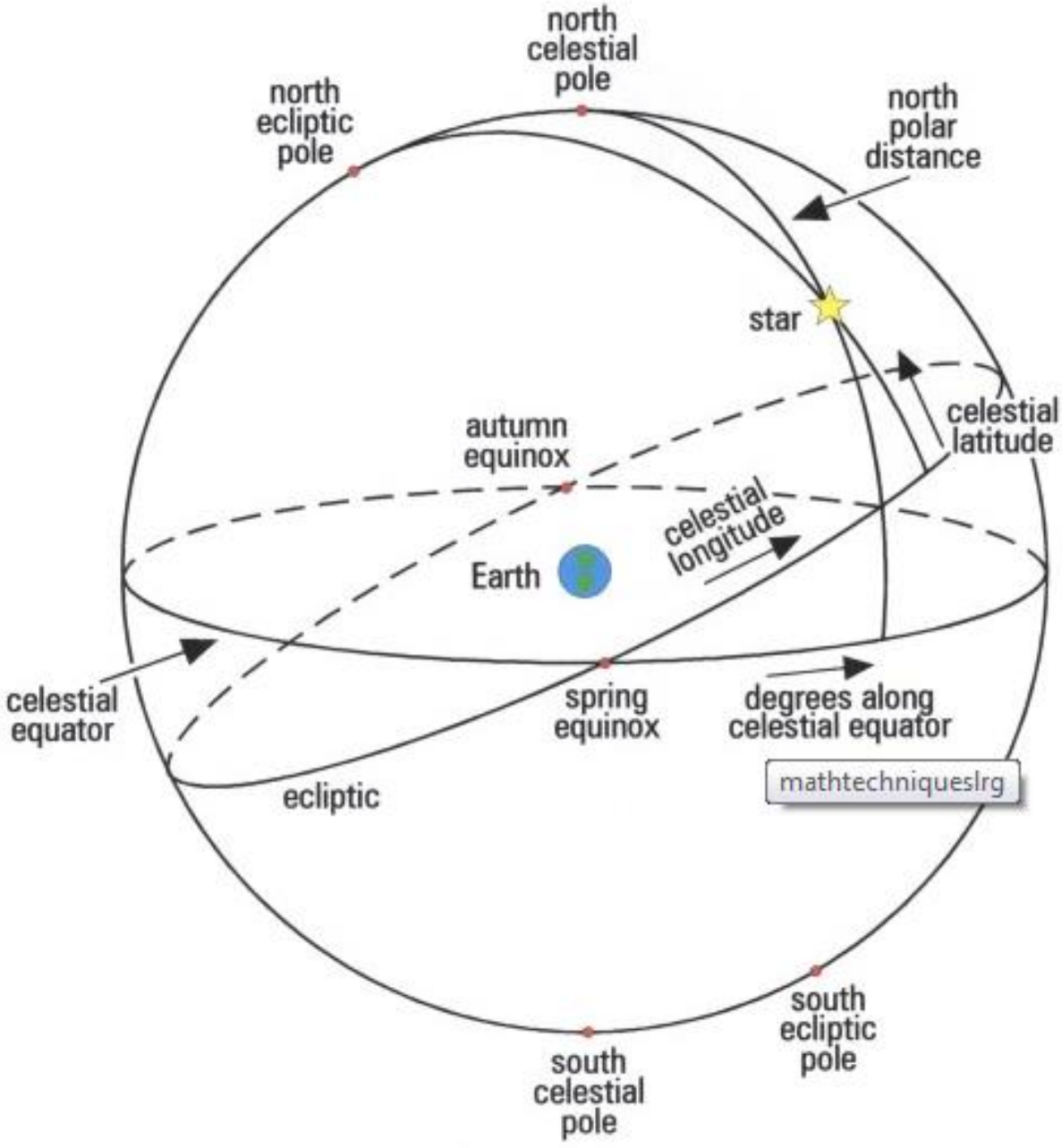

Fig.2.4 The ecliptic: the sun's annual path around the celestial sphere. The path is 23.45˚deviated from the celestial equator due to the tilt of the earth about its axis of rotation.

Source: https://elfindingpolaris.wordpress.com/the science-of-stars/

Solar time

Solar time is based on the apparent angular motion of the sun across the sky with solar noon as the time the sun is overhead an observer. This is the time the sun crosses the meridian of the observer. Solar time is used in all sun angle relationships and does not necessarily coincide with the local time. It is therefore necessary to carry out a conversion from the standard time to solar time.

Solar Time – standard Time = $4(L_{st} - L_{loc}) + E$ (2.3)

L_{st} is the standard meridian of the local time zone.

L_{loc} is the longitude of the observer

E is the Equation of time.

Equation of time

A solar day is the interval of time (not necessarily 24 hours) when the sun appears to complete one cycle about a stationary observer on earth. It varies in length throughout the year. The two principal factors for the variance being:

a. The earth sweeps out unequal areas on the elliptical plane as the earth's orbit is not circular but elliptical.
b. The earth's polar axis is tilted with respect to the elliptic plane.

The Equation of time can be represented thus:

$E = 229.2(0.000075+0.001868\cos B-0.032077\sin B-0.014615\cos 2B-0.04089\sin 2B)$ (2.4)

Where $B = \frac{360}{365}(n-1)$

or

$E = 9.87\sin 2\beta - 7.5\cos\beta - 1.5\sin\beta$ (2.5)

Where β = $\frac{360}{364}(n-1)$

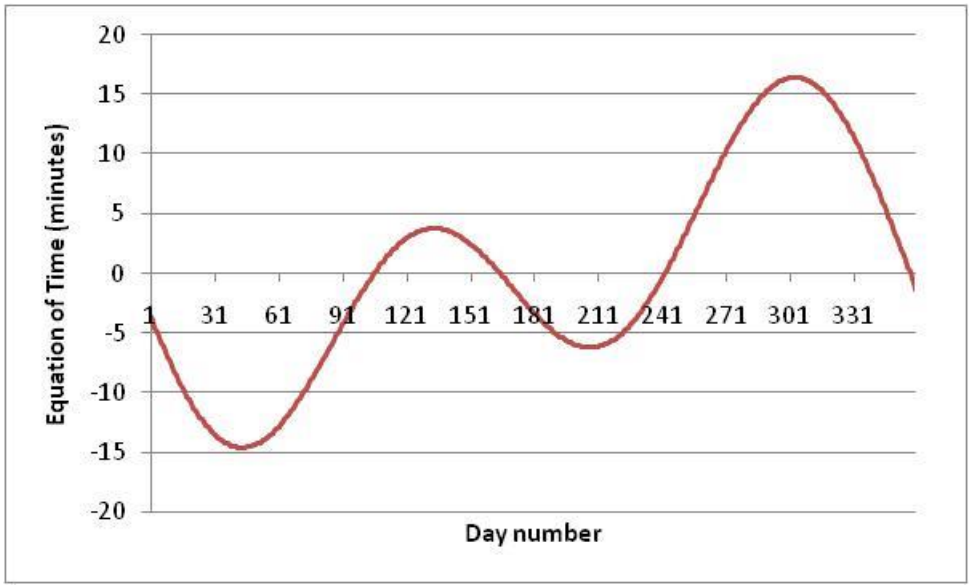

Fig.2.5 Variation of the equation of time over the year.

For the reader to appreciate the geometric relationships between a solar collector and the incoming beam of solar radiation, several angles need to be defined.

From the definitions given in the nomenclature, the angle of incidence, Θ of a beam of radiation on a collector surface tilted at angle β is given by:

cosΘ = sinδsinΦcosβ - sinδcosΦsinβcosϒ+ cosδc osΦcosβcosω+ cosδsinΦsinβcosϒcosω + cosδsinβsinϒsinω (2.6)

Or

cosΘ = cosΘ$_z$cosβ + sinΘ$_z$sinβcos(ϒ$_s$-ϒ) (2.7)

for a horizontal surface :

β = 0

$\Theta=\Theta_z$

$\cos\Theta z = \sin\delta\sin\Phi + \cos\delta\cos\Phi\cos\omega$ (2.8)

For a collector in the Southern Hemisphere facing North

$\Upsilon = 180^{\circ}$

$\cos\Theta = \sin\delta\sin(\Phi+\beta) + \cos\delta\cos(\Phi+\beta)\cos\omega$ (2.9)

at solar noon

$\Theta_{z\ noon} = [\Phi + \delta - \beta]_{magnitude}$ (2.10)

where:

Φ is the latitude of the collector

β is the tilt angle of the collector relative to the horizontal axis

Υ is the azimuth angle

Υ_s is the solar azimuth angle

ω is the hour angle

Zenith, Azimuth and Hour angles

Relative to a stationary observer the sun moves across the sky and the following angles need to be noted.

The angle of the sun relative to a line perpendicular to the earth's surface is the zenith angle Θ_z.

The sun's position relative to the North-South axis is the solar azimuth Υ_s.

Relative to the collector, the deviation of the projection on a horizontal plane of the normal to the collector surface from the local

meridian with zero due North, East positive and West negative is the surface azimuth ϒ.

The hour angle ω is the angular displacement of the sun east or west of the local meridian due to the rotation of the earth on its axis at 15˚ per hour with morning as negative and afternoon positive. At solar noon the hour angle is defined as zero when the sun is at its highest in the sky.

Sunrise and sunset times

Sunrise and sunset occur when the sun is at the horizon. By setting to 90˚ the zenith angle, cosine Θz is set to zero.

Sun set hour angle ω_s

$\cos\omega_s = - \sin\Phi\sin\delta/\cos\Phi\cos\delta$

$= -\tan\Phi\tan\delta$ (2.11)

Number of daylight hours is given by:

$N = \frac{2}{15} \times \cos^{-1}(-\tan\Phi\tan\delta)$

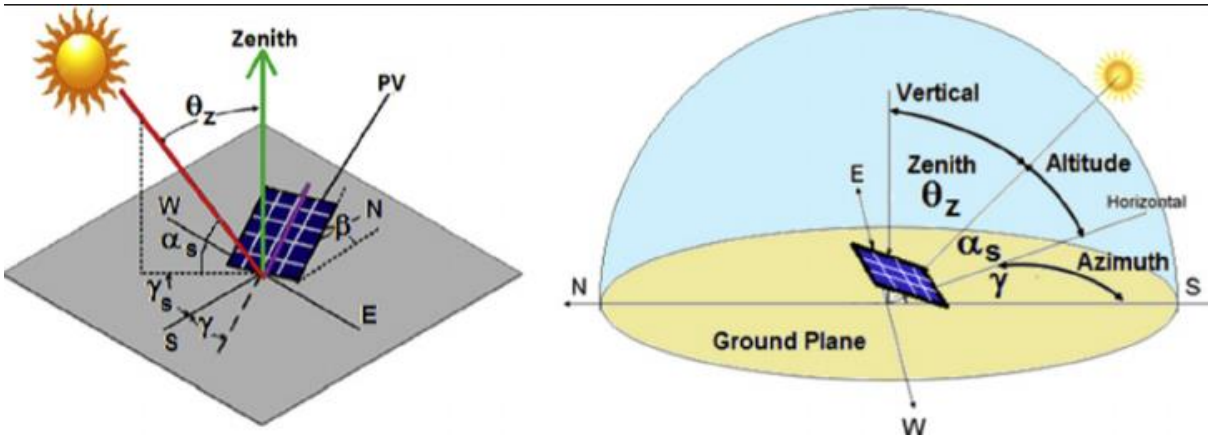

Fig.2.6

Various sun angle relationships for beam radiation

Source: www.e.education.psu.edu/

2.1.2 Terrestrial radiation

Solar thermal systems performance is measured on long term performance. There is therefore need for knowledge of long term monthly coverage daily insolation data for the locality under consideration. This information is available from radiation maps, meteorological services. Compiled data on global, diffuse and beam solar radiation over Zimbabwe and the locally developed model for estimation of diffuse radiation using local data is a major boost for solar radiation practitioners and scholars in Zimbabwe. Hove and Gottsche (1998)

Most radiation calculations are done using the normalized radiation levels that is the ratio of the pyranometer measured radiation, (H and I) to the theoretically available radiation if there was no atmosphere, (H_o and I_o). H and I are always less than H_o and I_o respectively due to attenuation caused by atmospheric albedo. This ratio is a measure of the clearness index. The clearness index can be a daily parameter or an hourly one.

To calculate the daily index the starting point is to integrate equation (1.1) from sunrise to sunset over a horizontal surface to obtain the daily radiation income.

$$H_o = \frac{24 \times 3600 G_{sc}}{\pi}\left(1 + 0.033 \cos \frac{360n}{365}\right) \times \left(\cos \phi \cos \delta \sin \omega_s + \frac{\pi \omega_s}{180} \sin \phi \sin \delta\right) \quad (2.12)$$

The daily clearness index is then obtained from the ratio:

$K_T = \frac{H}{Ho}$ (2.13)

Where H is obtained from pyranometric measurements.

Similarly to obtain an hourly index I_o the hourly radiation income is obtained by integrating the same equation over an hour long period.

$$I_o = \frac{12 \times 3600}{\pi} G_{sc}\left(1 + 0.033 \cos \frac{360n}{365}\right) \times \left[\cos \phi \cos \delta \left(\sin \omega_2 - \sin \omega_1\right) + \frac{\pi(\omega_2 - \omega_1)}{180} \sin \phi \sin \delta\right] \quad (2.14)$$

The hourly clearness index is calculated from the ratio of the measured hourly radiation I to the calculated hourly radiation I_O in the same hour if there was no atmospheric albedo.

The ratio $k_T = \frac{I}{Io}$ is then calculated. (2.15)

To estimate the daily diffuse component a number of models are available. Hove and Gottsche (1999) for daily diffuse radiation is one such formulation, Liu and Jordan (1960) and Bendt et al (1981) are others. In Zimbabwe the Hove and Gottsche has the advantage of having been generated with local data as researchers have questioned the universality of correlations generated from specific data. J.A Duffie and W.A Beckman page 74 4th Edition

For hourly diffuse component the Orgill and Hollands (1977), Erbs et al (1982) and Reindl et al (1990) are available correlations which are almost identical. In this research the Orgill and Hollands is used because the data used is suitable for hourly analysis and Orgill and Hollands is more widely used.

$I_d/I = 1.0 - 0.249k_T$ for $0 \leq K_T \leq 0.35$

$= 1.557 - 1.84k_T$ for $0.35 < k_T < 0.75$

$= 0.177$ for $k_T > 0.75$ (2.16)

I_d is calculated from the appropriate value of k_T

The beam component I_b is calculated as the complement of I_d that is

$I_b = I - I_d$ (2.17)

Another parameter, the geometric factor is defined as the ratio of beam radiation on a tilted surface to that of beam radiation on a horizontal surface at any one time.

$$Rb = \frac{Gbt}{Gb}$$

$$= \frac{Gbncos\Theta}{Gbncos\Theta z}$$

$$= \frac{cos\Theta}{cos\Theta z} \quad (2.18)$$

Knowing R_b the global radiation on a tilted surface can then be modelled using the Liu and Jordan model (1963) or the simplified Hottel and Woertz (1942).

The Liu and Jordan model (1963) can be represented as follows:

$$I_T = I_b R_b + I_d(1+\cos\beta)/2 + I_h\rho(1-\cos\beta)/2 \qquad (2.19)$$

The symbols are defined by the nomenclature used in the appendix.

The simplified Hottel and Woertz model can be represented as follows:

$$I_T = I_b R_b + I_d \qquad (2.20)$$

The Liu and Jordan will give more accurate results where ground reflectance is more pronounced. Otherwise the two models will give very close results as in this case where ground reflectance is 0.3 or less. For that reason the simplified Hottel and Woertz model was adopted in this research as it is simpler and gives almost identical results.

2.2 SOLAR WATER HEATING SYSTEMS

A solar water heating system (SWHS) combines a solar array, an energy transfer fluid and a storage tank. The heart of the solar water heater is the solar collector array which absorbs solar radiation and

converts it to heat. This heat is then absorbed by a heat transfer fluid that passes through the collector. The heat is then stored in a storage tank for use immediately or at a later stage.

For domestic water heating flat plate collectors are most convenient because of their low to medium temperature range which is typical for home usage. Their other advantage is that they are easily assembled and easy to operate. Their performance can be predicted in considerable detail with the aid of mathematical models.

In Zimbabwe solar water heaters are becoming very popular with home owners. In this regard the government has also put in place statutory mechanisms to encourage their usage under the name domestic solar geysers. The climate in Zimbabwe and the region characterised by bright sunshine days of relatively high irradiation intensities make solar water heaters an economic substitute to electric water heating in days of high and uninterrupted insolation. Kagande et al 2013 predict a solar fraction of 0.4 with one array with an absorber area of 1.81m^2 and a tank of 250 litre. They further predict SF of 0.78 with two arrays with drain off facilities.

Two types of solar water heating systems are available; these are the direct system and the indirect system. In the direct system the water is the transfer fluid and it is heated directly in the collector and transported to the storage tank. In the indirect the water is heated indirectly by a heat transfer fluid that is heated in the collector and passes through a heat exchanger to transfer heat to the domestic service water. Solar water heating systems can be viewed from the way the transfer fluid is transported. These are the passive systems or natural systems known as the thermosiphon or the forced circulation or pumped system.

2.2.1 The thermosiphon system

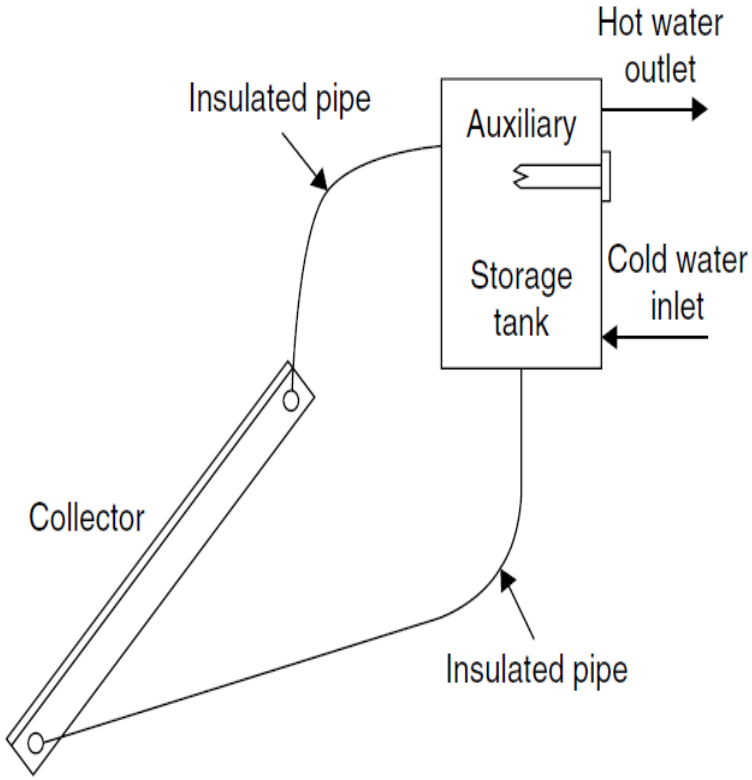

Schematic diagram of a thermosiphon solar water heater.

Fig.2.7 Source:Kalogirou (2009):253

The thermpsiphon is a heat exchange method based on natural convection which circulates the fluid without the need of a mechanical pump. The system can either be direct or indirect. In the

direct system the transfer fluid is water which is the same fluid in the storage tank. In the indirect system the transfer fluid is transfers the heat to the water in the storage tank through the medium of a heat exchanger. Heated fluid rises in the loop as it is less dense than cooler fluid. The temperature gradient gives rise to a density gradient resulting in natural convection. A good thermosiphon has little hydraulic resistance so the liquid will flow easily under the relatively low pressure produced by natural convection. The system is simple relatively less expensive. In thermosiphon systems the tank has to be situated higher than the collectors and all the pipe work to rise gradually from the furthest collector to the storage tank. In order to reverse circulation at night a thermal diode is usually installed. Kong Seng Ong et al (2014) showed through experiments that it is poor insulation of the tank and pipe work rather than reverse thermosiphon that is responsible for significant heat loss at night.

Advantages of thermosiphon system;

- It contains no electrical components.
- It is reliable and easy to maintain
- It has a longer life span than active systems.

2.2.2 Pumped system

Pumped system can be indirect or direct. The major difference just like in the thermosiphon is that in the latter case the heat gained by the collector loop is not transferred directly to the contents of the storage tank but via a heat exchanger. This entail using different heat transfer fluid to the fluid contained in the storage tank. The mathematical model representation for the solar collector combined with a heat exchanger is exactly like a collector alone with a reduced heat removal factor F_R. Kalogiou (2009) pp 258. Although the indirect system is not as efficient as the direct system due to performance

losses caused by the heat exchanger they have other advantages over the direct systems. These are:

- The possibility of selecting a suitable fluid with low freezing point can increase the range of operation to cater for countries with freezing temperatures. Selection of a fluid with high boiling point can prevent damage caused by boiling.
- Corrosion of collector components can be controlled by use of corrosion inhibiting transfer fluid.
- Built up of lime in the collector components can be prevented by the use of a suitable transfer fluid. The lime can be displaced to areas that are cleaned more regularly.
- Cheaper materials can be selected for the collector and piping materials.

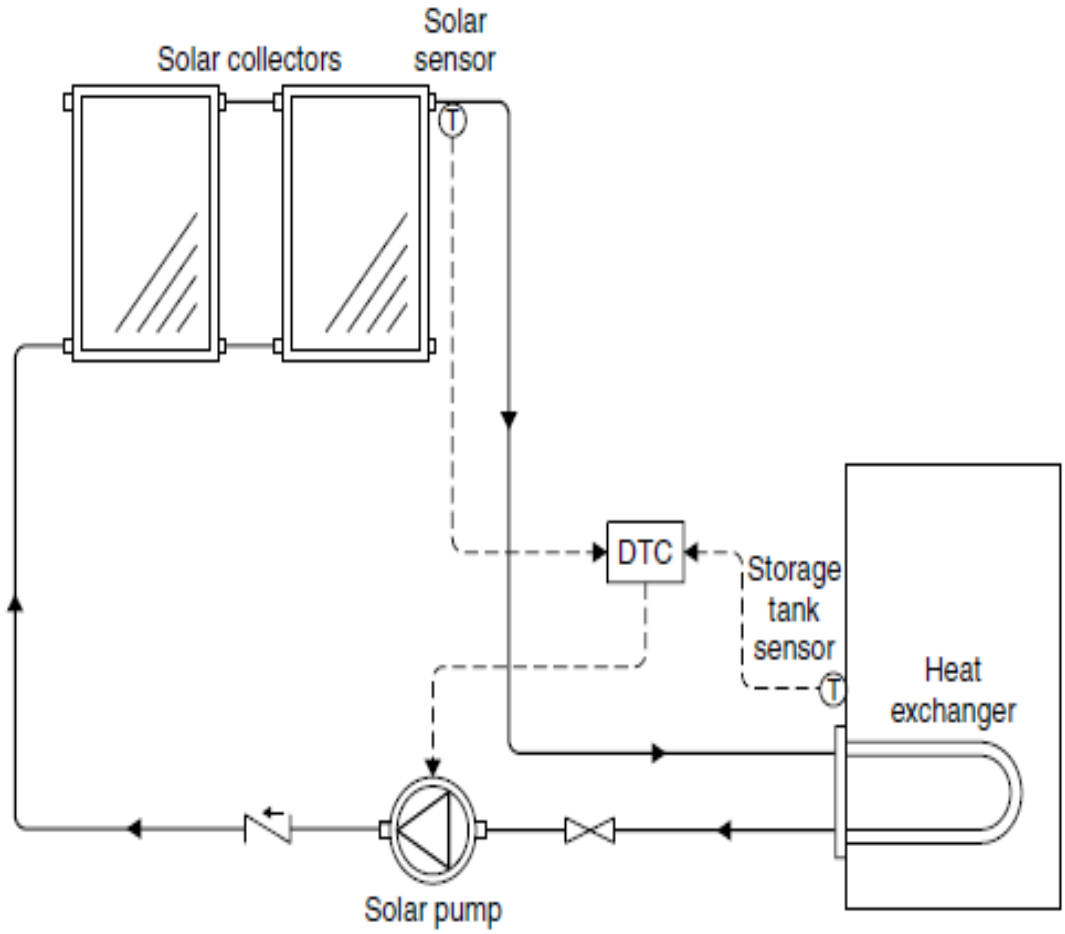

Fig.2.8

Pumped indirect system with Differential Temperature Controller (DTC)

Source: Kalogirou (2009):299

In the pumped system the fluid is pumped through the collector and into the storage tank heat exchanger. The pump is controlled by a DTC differential temperature controller which switches the pump on

and off. The DTC monitors the temperature difference between the collectors and the storage tank. When the temperature difference exceeds the set point the controller switches the pump on. When the temperature difference falls below the set point the controller switches off the pump.

2.3 THEORY OF FLAT PLATE COLLECTORS

A flat plate collectors (FPC) is a special type of heat exchanger that transforms solar radiant energy into useful heat. Whereas a conventional heat exchanger accomplishes fluid to fluid heat exchange with radiation playing an insignificant role, the solar collector transforms heat from the sun's radiation into useful heat to be stored for use immediately or a later stage. The wavelength of the radiation involved is of the short range from 0.3 to 3µm which is much shorter than the emitted radiation from most heat absorbing surfaces. The flux of incident radiation is at best around 1100W/m^2 and is variable. The analysis of solar collectors therefore takes into account the low and variable energy fluxes and the prominent role of solar radiation.

FPC's are designed for applications requiring energy delivery at moderate temperatures of up to around 100˚C above ambient temperature. They use both beam and diffuse solar radiation and do not require tracking of the sun. Little maintenance is required as its structural construction and mode of operation is static. The solar flat collector has as its major attraction the simplicity of its mechanical construction. The major applications are in solar water heating, space heating, air conditioning and industrial process heating. Passive heating of buildings can be viewed as special cases of FPC with the room or storage wall as the absorber.

The theory of FPC is fairly well developed. The main features of its construction are as in figure 2.9

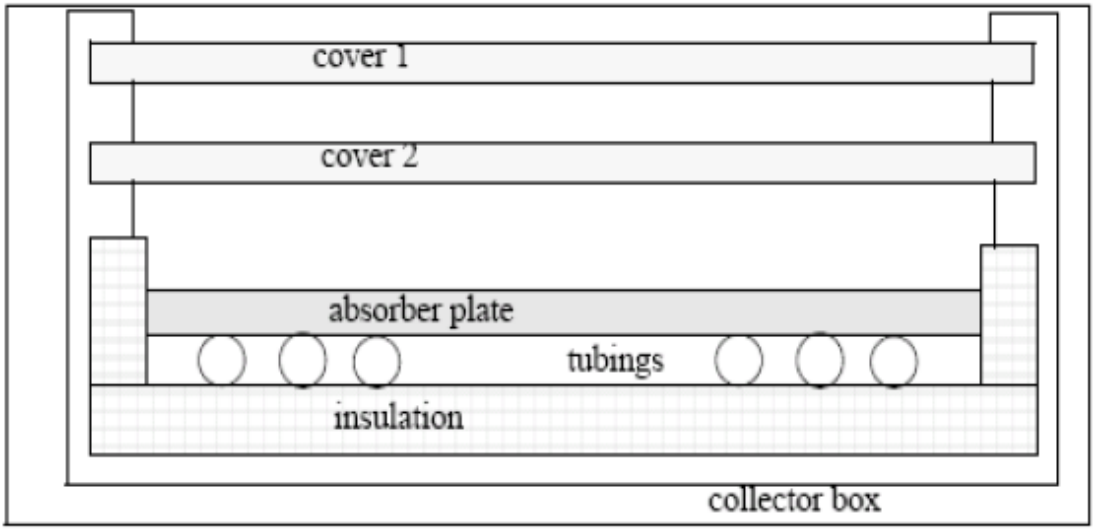

Fig.2.9 Cross section of a basic flat plate collector with two covers

Source: Hamidi S.T. (2011)

Absorber plate: this is a plate coated with a selective absorption material which absorbs short wave radiation and transmits long wave radiation to the transmitting fluid.

Glazing: is made of glass or plastic which is transparent to solar short wave radiation but opaque to long wave infrared radiation thereby reducing heat losses due to radiation and convection to the surrounding environment.

Back and edge insulation is designed to reduce conduction losses.

FPC are mounted in a stationary position to form an integral part of the roof or other structure. The orientation is optimised for a particular location for the time of the year in which the device is

intended to operate. In all cases the collector must face the equator that is north facing for the southern hemisphere and south facing for the northern hemisphere. Kalogirou (2009) suggest that depending on the application for solar cooling then the optimum tilt is latitude - 10˚ so that the sun will be perpendicular to the collector during summertime when the energy will be mostly required. If the application is space heating then the optimal angle is latitude +10˚, whereas for annual hot water production it is latitude +5˚ to have relatively better performance during wintertime when hot water is mostly required but not ignoring other months.

Energy balance

Fig 2.10

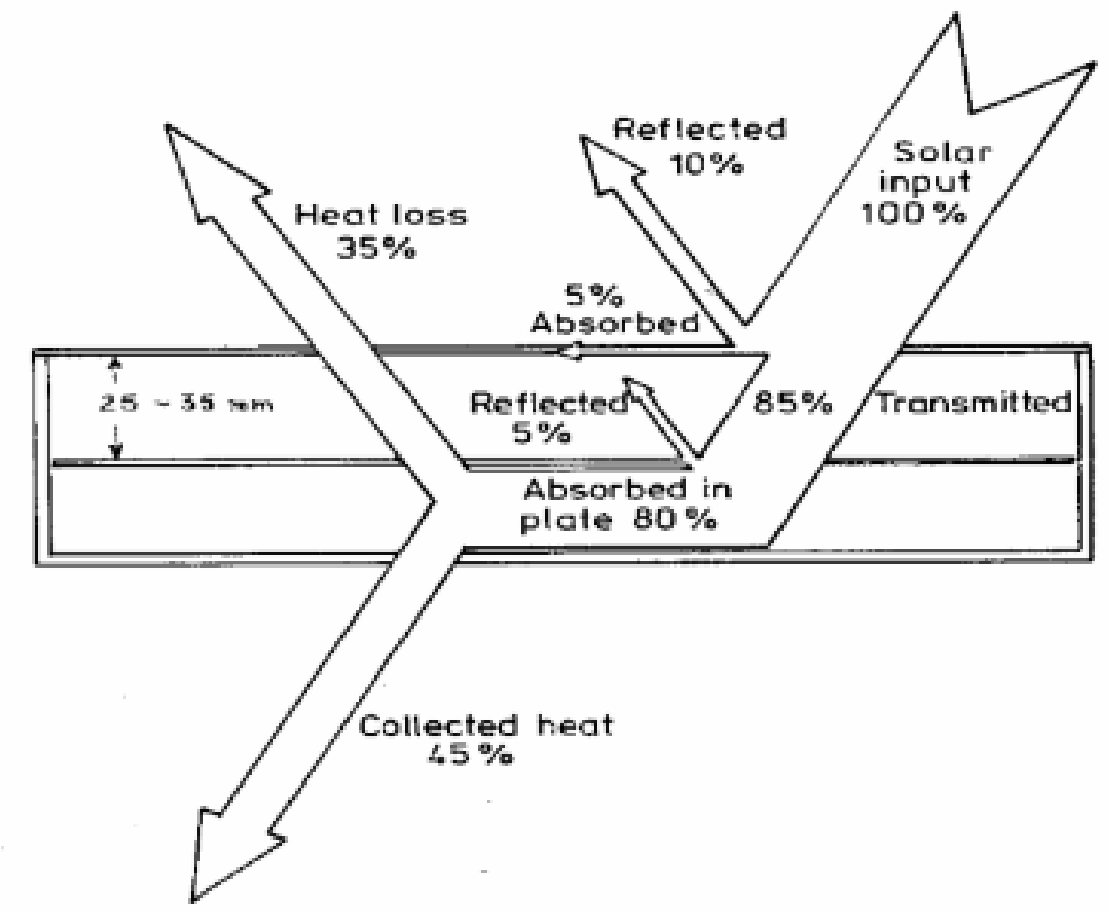

Source: Struckman F(2008)

If G_T is the intensity of solar radiation on the tilted surface in W/m^2 incident on the aperture plane of the solar collector having collector surface A_C in m^2 then the amount of solar radiation received by the collector is Q_i where

$$Q_i = A_C G_T \quad (2.21)$$

From fig.3.2 part of the radiation is reflected back to the sky, another component is absorbed by the glazing and the rest is transmitted through the glazing and reaches the absorber plate as short wave radiation. The transmission factor ʈ and the absorption factor α form the conversion factor ʈα.

$$\text{Thus } Q_i = A_C G_T \tau\alpha \quad (2.22)$$

As the collector absorbs heat its temperature rises above that of the ambient and heat is lost by convection and radiation. The rate of heat loss Q_O depends on the heat transfer coefficient U_L and the temperature difference between the collector and the ambient.

$$Q_O = U_L(T_C - T_a) \quad (2.23)$$

Some energy is stored in the collector at a rate Q_S but these are transient effects which in the course of the day are very small and can be considered too small compared to Q_i and Q_O. International Energy Agency (IEA), Solar Heating and Cooling Programme (1993) report.

The useful energy extracted by the collector Q_U expressed as a rate of extraction is therefore reduced under steady state conditions to the difference of only two terms.

$$Q_U = Q_i - Q_O \quad (2.24)$$

$$Q_U = A_C G_T \tau\alpha - U_L(T_C - T_a) \quad (2.25)$$

The collector temperature is difficult to measure and is a function of the collector design. It is therefore desirable to reformulate the above equation so that the useful energy gain can be expressed in

terms of the inlet fluid temperature and a parameter called the heat removal factor F_R which can be evaluated analytically or can be measured. F_R is defined as the ratio of the useful energy gain of a collector to the useful gain if the whole collector surface were at the fluid temperature. The heat removal factor accounts for the fact that the fluid entering the collector is heated in the direction of flow and consequently is not all at the same temperature as the inlet fluid. IEA (1993) report.

$$F_R = Mcp(T_i - T_a)/A_C[G_T \tau\alpha - U_L(T_i - T_a)] \quad (2.26)$$

Rearranging equation (3.6)

$$Mcp(T_i - T_a) = F_R A_C[G_T \tau\alpha - U_L(T_i - T_a)$$

$$Q_U = F_R A_C[G_T \tau\alpha - U_L(T_i - T_a) \quad (2.27)$$

2.3.1 Flat Plate Collector Efficiency

A useful parameter to express the performance of a FPC is the collector efficiency η. It is defined as the ratio of the useful energy gain Q_U to the incident solar energy over a particular time period. The instantaneous efficiency is given by:

$$\eta_{coll} = F_R A_C[G_T \tau\alpha - U_L(Ti - Ta)]/A_C G_T \quad (2.28)$$

$$\eta_{coll} = F_R \tau\alpha - F_R U_L(Ti - Ta)/G_T \quad (2.29)$$

Looked at from the energy gain by the water the efficiency can also be expressed as the ratio of the energy gain by the water to the radiant energy incident on the collector over a given time period.

$$\eta = Mcp(T_i - T_a)/\Delta t G_T A_C \quad (2.30)$$

Equation (2.27) is known as the Hottel-Whillier-Bliss equation and is the basis for formulating performance parameters for solar collectors. To make the units of U_L in Joules per second compatible with those of $G_T \tau\alpha$ in Joules per m^2 per hour, U_L must be multiplied by 3600 to convert the units to Joules per hour.

2.3.2 Incident Angle Modifier

Another important aspect on collector theory is the determination of the effects of the angle of incidence of the incident radiation. The performance equation (2.29) assumes that the sun is perpendicular to the plane of the collector which rarely occurs thereby reducing the ($\tau\alpha$) product. The transmittance τ is most affected by the angle of incidence Θ than the absorbance factor α. Kalogirou (2009). The incidence angle modifier K_Θ is defined as the ratio of the transmittance absorbance product $\tau\alpha$ at any angle of incidence Θ to the transmittance absorbance product at normal incidence $(\tau\alpha)_n$

$$K_\Theta = \tau\alpha/(\tau\alpha)_n \qquad (2.31)$$

Hence $\tau\alpha$ at any angle of incidence is the product of $\tau\alpha$ at normal incidence times the incidence modifier at that angle of incidence.

A general expression suggested by Sauka and Safwat(1996) for angular dependence of KΘ for collectors with flat covers is:

$$K_\Theta = 1 - b_o\left(\frac{1}{cos\Theta} - 1\right) \qquad (2.32)$$

The coefficient b_o is estimated at b_o=0.136. for Θ less than 60˚ the equation is fairly accurate.

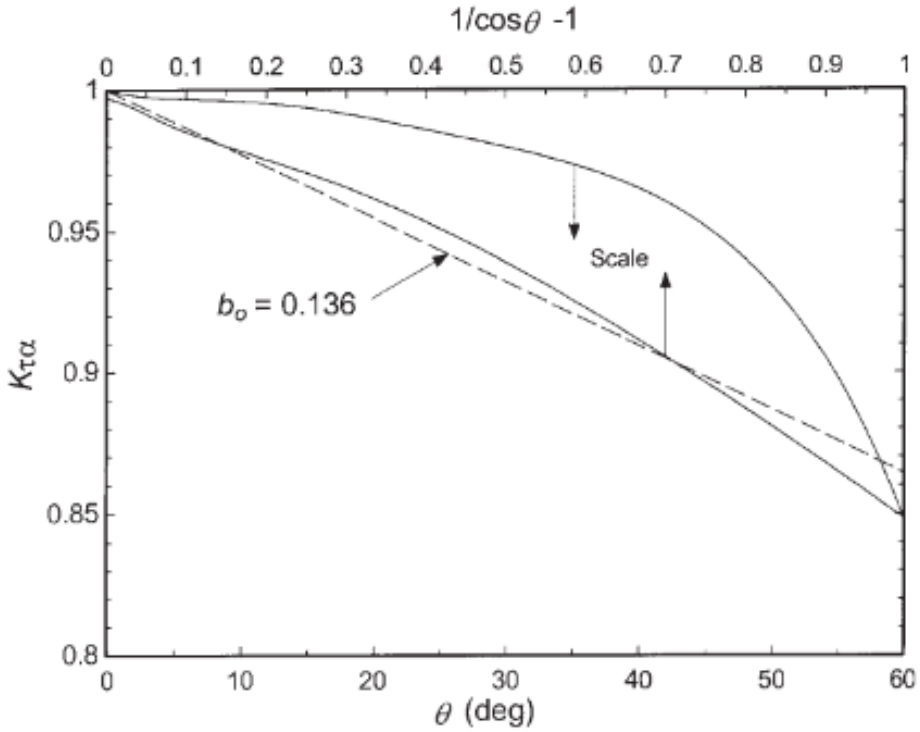

Fig.2.11 Incidence angle modifier as a function of Θ and (1/cosΘ)-1 for a collector with a flat cover.

Source: Duffie (2013)

The collector efficiency equation can then be written for any incident angle as:

$\eta_{coll} = F_R(\tau\alpha)nK_\Theta - F_RU_L(Ti-Ta)/G_T$ (2.33)

$\eta_{coll}/K_\Theta = F_R(\tau\alpha)_n - F_RU_L(Ti-Ta)/G_TK_\Theta$ (2.34)

Plotting (η/K_Θ) vs $(Ti-Ta)/G_TK_\Theta$

Will yield a straight line with intercept of $FR(\tau\alpha)_n$ on the y-axis and gradient $-F_RU_L$

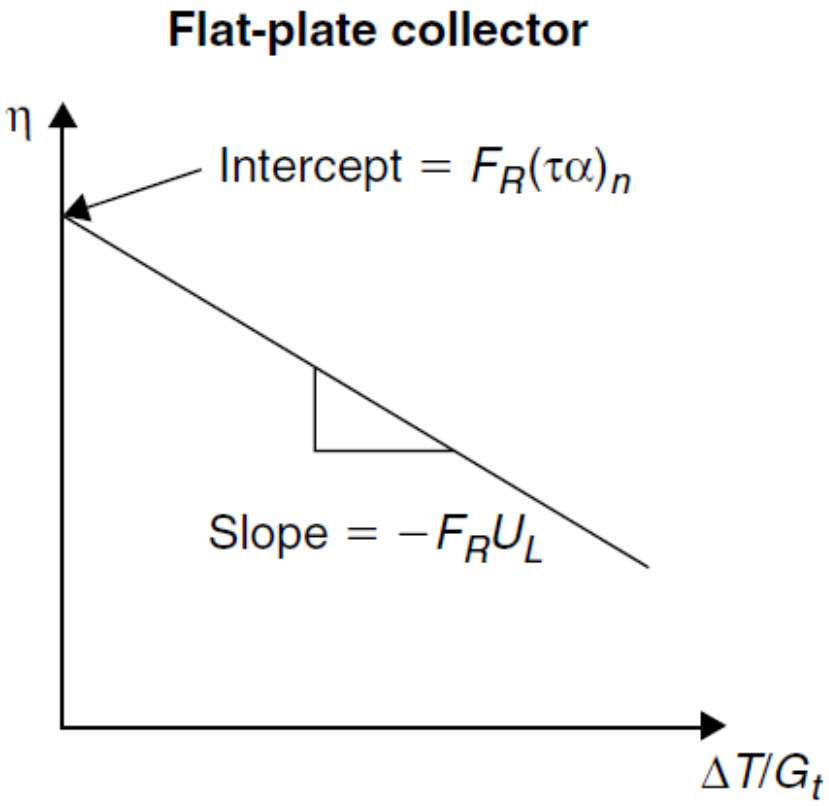

Fig.2.12 graph showing gradient and y-axis intercept of η vs $\Delta T/G_t$

η is maximum when Ti =Ta

and $\eta = F_R(\tau\alpha)_n$

At the intersection with the horizontal axis the collector efficiency is zero. At this condition it is either, there is such low level of radiation or such high fluid temperatures that heat losses equal solar absorption and the collector delivers no useful heat. This is the stagnation temperature and occurs when no fluid flows in the collector. This maximum temperature for a FPC is got by setting η= 0 in the efficiency equation and gives; Duffie (2013)

$T_{max} = G_T(\tau\alpha)_n/U_L + Ta$ (2.35)

2.4 Thermal Analysis of storage Tanks

Although the storage tank is an integral part of the solar water heating system it is important to briefly treat it separately to bring out the heat transfer mechanisms that take place. More so the evaluation of the tank heat loss coefficient has to be done separately from the temperature decay that takes place after sunset in the absence of solar radiation.

For a fully mixed or stratified storage, the thermal capacity Qs of a liquid storage unit at uniform temperature operating over a finite temperature difference ΔT, is given by the thermal equation:

$Qs = MCp\Delta Ts$ (2.36)

M = mass of storage capacity

Cp = specific heat capacity of storage fluid (water)

Energy balance of the storage tank.

$McpdTs/dt = Q_U – Q_L - Q_{loss}$ (2.37)

Q_U = rate of collected solar energy delivered to the tank

Q_L = rate of energy removed from the storage tank to the load

Q_{loss} = rate of energy loss from the storage tank to the ambient

The rate of storage tank energy loss is given by

$Q_{loss} = UA_s(Ts-Ta)$ (2.38)

Where UA_s = storage tank loss coefficient and area product in W/˚C

T_a = temperature of ambient where the tank is located.

To determine the long term performance of the storage tank (4.2) may be rewritten in finite difference form as:

$T_{s-n} = T_s + (\Delta t/Mcp)[Q_U - Q_{loss} - (UA_s)(T_s - T_a)]$ (2.39)

Where Ts-n = the new storage tank temperature (˚C) after time interval Δt. this equation assumes that the heat losses are constant in the period Δt. Kalogirou 2009

In this research the storage tank loss coefficient and area product was evaluated from the temperature decay when there was no radiation and no energy was taken to the load.

$Mcp\Delta Ts/\Delta t = UAs(Ts-Ta)$

$\Delta Ts/(Ts-Ta) = UAs\Delta t/Mcp$

Integrating :

$Ln(Ts_{beg}-Ta_{beg}) - Ln(Ts_{end}-Ta_{end}) = (UAs/Mcp)(t_{end}-t_{beg})$ (2.40)

Where:

Ts_{beg}=Temperature of the storage tank at the beginning of an interval

Ta_{beg}= Temperature of the ambient at the beginning of an interval

Ts_{end} =Temperature of the storage tank at the end of an interval

Ta_{end} = Temperature of the ambient at the end of an interval

For evaluating the value of UA_s in (4.6) Ts_{beg} and Ta_{beg} are averages of the respective values in that interval. J Burch and L Magnuson (2009)

CHAPTER 3

3.1 Methodology

Theoretical framework

From chapter 2, it was shown that the basis of solar collector characterisation was bases on the Hottel-Whillier-Bliss equation equation (2.27).

$Q_U=A_C F_R[G_T(\tau\alpha)_n K_\Theta - U_L(T_i-T_a)$

With the notation illustrated earlier. From the above equation the thermal efficiency was derived by dividing both sides of the equation by the energy input $A_C G_T$. (2.29)

$\eta= F_R(\tau\alpha)_n K_\Theta - F_R U_L(T_i-T_a)/G_T$

in this case the tilt angle of the collector was set at 37.5˚ by the manufacturer and is therefore not optimised at Harare latitude 17.8˚S. it is therefore necessary to include the Incidence angle modifier term K_Θ.

By dividing both sides of the equation by K_Θ it becomes possible to include the incidence angle modifier term in the parameters for evaluating the optical efficiency as well as the environmental parameters T_a,G_T as well as the fluid temperature T_i.

$\eta/K_\Theta = F_R(\tau\alpha)_n - F_R U_L(Ti-Ta)/G_T K_\Theta$

This is the collector characterisation equation. In this study the solar water heating system comes as a complete system where it is not possible to isolate the collector and storage tank as well as provide the instrumentation for measuring inlet fluid temperature and the flowmeter for measuring fluid flow.

Fig.3.1

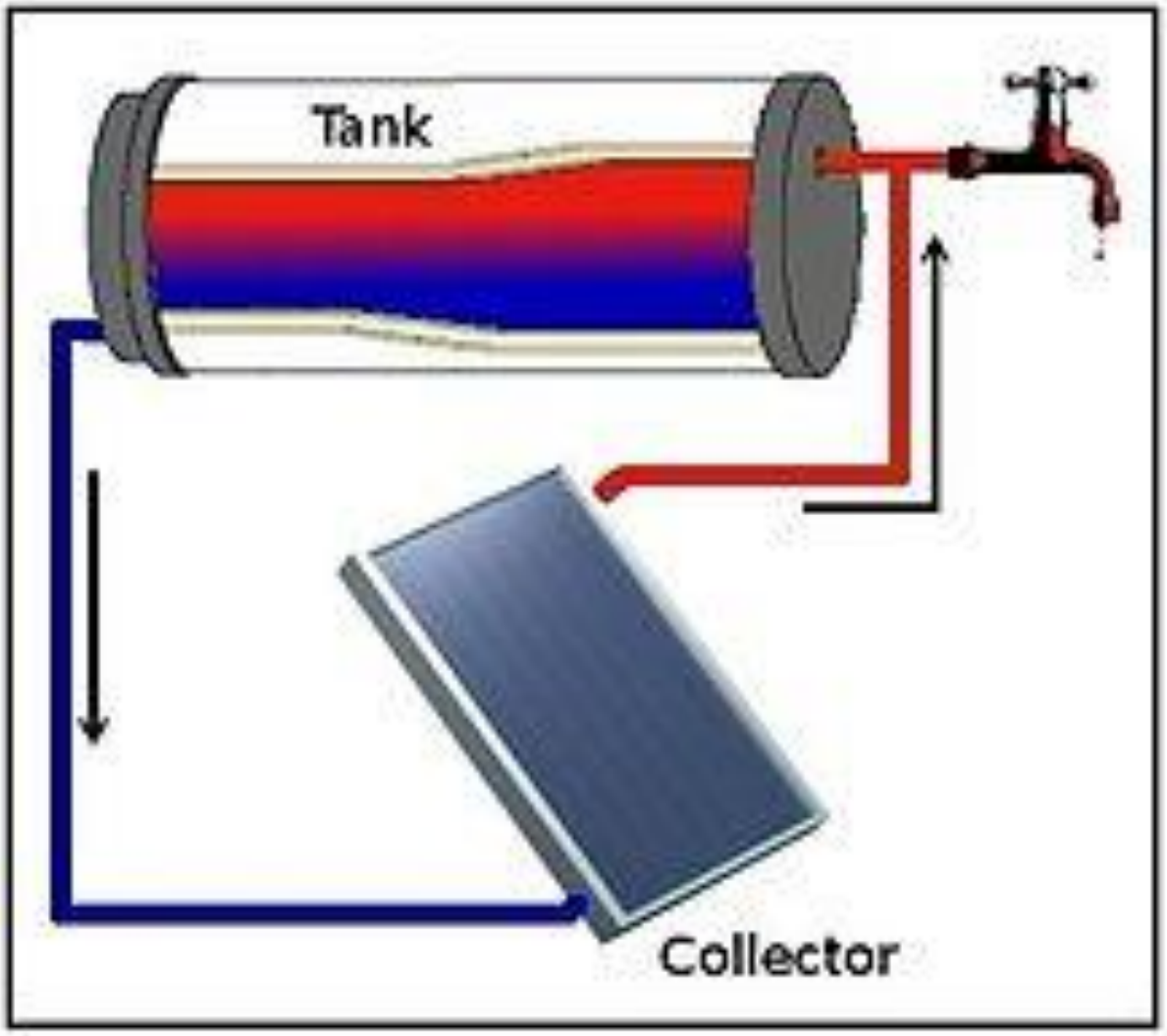

Fig.3.1 Collector storage tank system

Source: wikipedia

For the collector-storage tank system the useful energy gain is derived from the Hottel-Whillier-Bliss equation where the storage tank temperature is taken as the surrogate temperature for the inlet fluid temperature for the collector. This is an approximation as this is not the temperature that the collector is “seeing.” If a factor of heat

taken to the load by drawing hot water is included, the general equation for useful heat gain becomes;

$$Q_U = A_C F_R(G_T(\tau\alpha)_n K_\Theta - U_L(T_s - T_a) - \dot{m}_L Cp(T_s - T_{mu}) - UA_s(T_s - T_a) \quad (3.1)$$

$\dot{m}$ is the load constant flow rate, T_{mu} is the make-up water constant temperature. During characterisation stage and validation stage of this study there was no load so the middle term involving $\dot{m}$ is zero.

The energy gain in a water heater system can then be reduced to;

$$Q_U = A_C F_R(G_T(\tau\alpha)_n K_\Theta - U_L(T_s - T_a) - UAs(Ts - Ta) \quad (3.2)$$

Dividing by the energy incident on the collector $A_C G_T$ to get the efficiency;

$$\eta = F_R(\tau\alpha)_n - (F_R U_L + U_s A_s / A_C)(T_s - T_a)/G_T K_\Theta \quad (3.3)$$

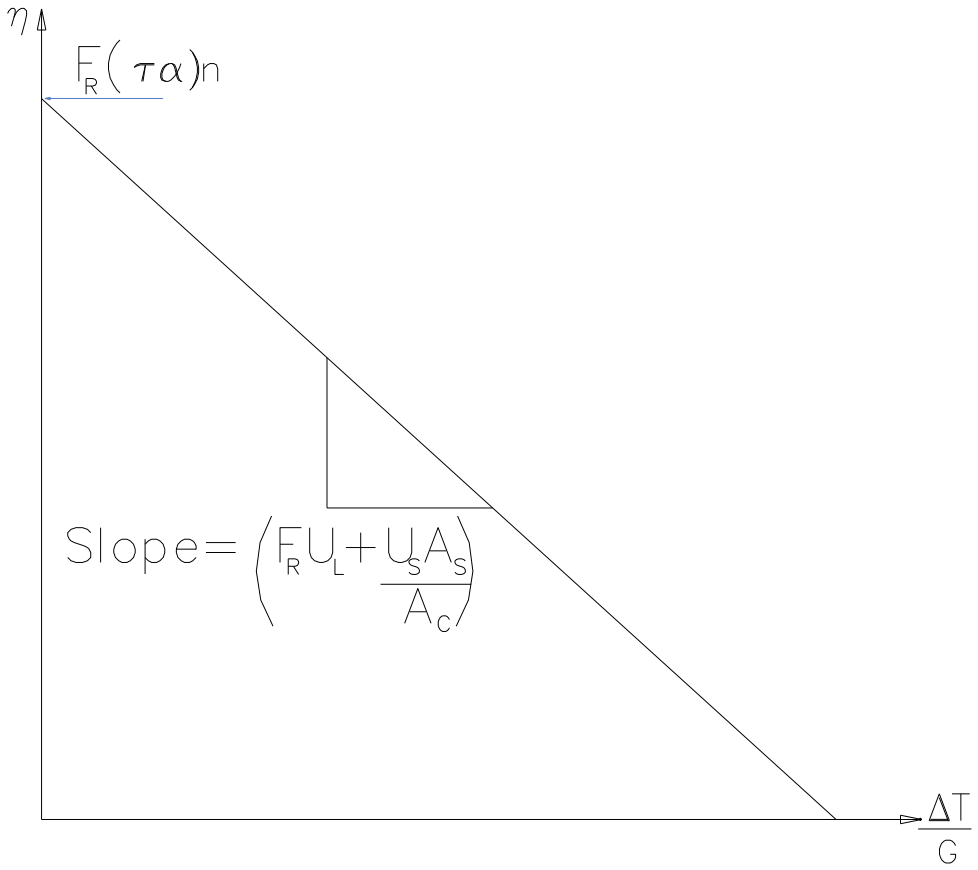

Fig.3.2 Collector storage tank system η vs $\Delta T/G_T$ graph

The rate Q_U is expressed as $\dot{m}Cp\Delta T$ with the usual notation. In this study there are no flowmeters to measure flowrates so mass rate is

exchanged for energy rate. The purpose of this research is to establish whether by expressing the energy rate in terms of the temperature rate dTs/dt it is possible to write the Hottel-Whillier-Bliss equation in that manner and go further to characterise the optical parameters and the heat loss parameters. The virtue of this method is the simplicity coupled with reduced need for more instrumentation.

Writing the energy balance equation as a differential first order equation:

$$MCpdTs/dt = A_C F_R G_T(\tau\alpha)K_\Theta - (F_R U_L + U_s A_s/A_C)(T_s - T_a) \qquad (3.4)$$

The expression can also be expressed in finite difference terms;

$$(MCp)(T_s^{n+1} - Ts^n)/\Delta t = A_C F_R G_T(\tau\alpha)K_\Theta - F_R U_L(T_s - T_a) - UA_s(T_s - T_a) \qquad (3.5)$$

The predicted temperature can be expressed as below.

$$T_s^{n+1} = Ts^n + A_C/MCp[F_R G_T(\tau\alpha)K_\Theta - (F_R U_L + U_s A_s/A_C)(T_s^n - T_a^n)]\Delta t \qquad (3.6)$$

Where Ts^{n+1} is the new storage tank temperature in (˚C)

T_s^n is the previous storage tank temperature.

T_a^n is the previous ambient temperature Kalogirou (2009)

The other symbols carry their usual notation as indicated earlier.

The theoretical framework outlined assumes that the storage tank temperature is the inlet fluid temperature of the collector. This assumption neglects the stratification that occurs in a storage tank especially on whose fluid is driven naturally by thermal syphon effect. Thermal syphon results in the lower strata being at lower temperatures than the average tank temperature. The upside of this effect is that as fluid from lower strata enters the collector inlet at lower temperatures than the average fluid temperature in the tank, it has the effect of improving the efficiency of the collector as this

effectively lowers the term $F_R U_L(T_s-T_a)/G_T$ in the efficiency equation. Kalogirou(2009)

The main assumption of this theoretical framework is to take T_s as the surrogate inlet fluid temperature in the collector. This is not wholly true as indicated earlier the collector is "seeing" a temperature which is lower than the average fluid temperature in the tank. The second assumption is to ignore mass transfer generated by thermosiphon effect and assume that heat transfer is the dominant process. The weakness of this assumption is that experiments have been carried out and demonstrated that F_R is not really constant but increases with increase in fluid flow. Kalogiruo (2009). One would therefore expect that the assumption will understate the value of F_R. A fluid in motion has been shown to remove more heat from the absorber plate than a stationery or near stationery fluid.

This theoretical framework replaces the mass flow rate $\mathring{m}$ with the temperature rate dT_s/dt in the energy useful gain equation. This is justified by the fact that the thermosiphon is a closed system such that the mass is constant over time but the temperature changes over time. One would also expect that at lower temperatures the heat removal would be more effective as a result of a larger temperature gradient between the absorber plate and the inlet fluid than at higher fluid temperature when this temperature gradient would be reduced. In other words the heat removal factor F_R from this model would be closer to the one from the mass flow model at low temperatures than at higher temperatures.

3.1 Procedure

The Solar Trailer

This study was carried out by making use of the solar trailer stationed at the faculty of engineering of the University of Zimbabwe. This particular unit is a donation by the Austrian Development Agency to the University. The solar trailer is a comprehensive solar unit essentially designed for training purposes in solar technology. The system is equipped with solar water heating systems; one of the thermosiphon type and the other of the forced flow type.

The thermosiphon system is equipped with a frame collector of the type RKE 2500 EASY, a domestic hot water tank (DHWT) of 150L capacity of type Kwiksol. The tank is integrated with a heat exchanger. The heat transfer fluid is propylene glycol, an antifreeze. The collector is mounted on a frame at 37.5˚ and is non-adjustable. There are temperature sensors to measure temperature of the collector, temperature of the storage tank and temperature of the ambient.

The forced flow system supplies hot water to a 300L compact hot water tank (CHWT). For comfort to the room the forced flow system is equipped with a set of Orion type radiators for space heating. The CHWT is connected to a solar station SST25 with a capacity to connect up to 25$m^2$of solar collectors to the hot water tank. This controller works with 3 Pt1000 sensors which control collector and tank temperatures as well as regulate the charge pump. Two solar thermal panels that deliver heat to the CHWT are located at the roof of the trailer with an adjustable angle of tilt from horizontal to 25˚. Radiation sensors are located on these roof top panels. These are the only radiation sensors for the whole trailer. Radiation measurement for the thermosiphon system are also taken from these panels.
SEG Mobile Training Centre manual (2014)

For lighting and electric power supply to accessories like measuring equipment and pumps, the solar trailer is equipped with solar photovoltaic panels, batteries, an inverter and voltage regulator.

3.2 Safety Procedures

The first step is to read the manual and understand safety and operational procedures. The study was limited to the thermosiphon system but it is necessary run the pumped system as well since the solar collectors for the pumped system need to be receiving radiation from which the radiation on the thermosiphon is modelled. Though the parameters on the forced flow system were not needed in this study it is necessary to keep an eye on them to the extent that allowable safe working parameters like allowable safe operating temperature of 95˚C is not exceeded and working pressure of 10bars is not exceeded. The system should only be allowed to operate between ambient temperatures of +2˚C to +40˚C. Before exposing collectors to solar radiation it is important to ensure that the tanks are filled with water to protect the equipment from excessive heat.

CHAPTER 4

4.1 Data collection.

After ensuring that both tanks are filled with water to the maximum the solar panels at the roof top are uncovered to allow radiation to be sensed by sensors S5. The collector for the thermosiphon is taken outside by means of its sliding mechanism. The charge- over switch is set to solar (2). The thermosiphon part of the solar water heating system is not equipped with data loggers so all the measurements were taken manually.

Readings for the local standard time, ambient temperature T_a (˚C), storage tank temperature T_s (˚C), radiation flux G (W/m^2) are recorded and tabulated as in tables 4.1, 4.2, 4.3 and 4.4. the readings were taken in intervals of 15 minutes. Any shading that occurred was measured with a tape measure so that the net collector area participating in radiation capture could be calculated.at each stage.

The day and year of the experiment is recorded at the top of the table. The readings were taken from 08:00 hours to 17 hours for radiation and temperature measurements. For the temperature decay of the storage temperature after sunset the readings were

taken up to mid night. For the full validation of temperature prediction results the readings were taken round the clock.

4.2 Sample calculations

The values used to fill in the Tables 4.1, 4.2, 4.3 and 4.4 are calculated using the relations that have been illustrated in the earlier chapters. For clarity to the reader, sample calculations are shown in the following pages to show how values in the tables are arrived at and eventually how the mathematical model for characterising the solar water heating system is evaluated.

Declination angle δ

Measurements were done on 22 April, 2017.

Day number (n) for 2 April

n = 92 that is (31+28+31+2)

the declination angle δ for 2 April is calculated using equation (1.2)

$\delta = 23.45\sin(360\frac{284+n}{365})$

$= 4.41^{\circ}$

At the university of Zimbabwe the latitude is 17.8˚S (-17.8)

The longitude is 31.03E (-31.03)

In all radiation calculations as stated earlier it is important to use solar time.

Applying equation (1.3) to calculate the solar time:

Solar Time (ST) = Local Time (LT)+ $4(L_{st}-L_{loc})$ +E

For local time of 12:00 the solar time is calculated on this day.

Solar time = 12:00 +4[(-30)-(-31.08)] +E

= 12.00 + 4.12 + E

E = 9.87sin2β-7.5cosβ-1.5sinβ

Where β=360/364(n-81)

β=10.879

E= -3.99

Solar noon =12.00 +4.12-3.99

=12.00 +(0.13)min

In Harare on 2 April the solar time and standard time has a difference of 7.8 seconds. For practical purposes the solar time and standard time are equal.

Radiation on tilted plane

The solar collector is tilted at 37.5˚ facing North that is ϒ=180˚

There is need to calculate the hourly clearness index K_T

For the hour 11:00 to 12:00 on 2 April

ω_1 = -15˚

ω_2 = 0˚

At 11:30, ω = -7.5˚

Applying equation (1.13) to get the radiation income in the hour 11:00 to 12:00;

$I_o = 12x3600xG_{sc}x1/\pi(1+0.033\cos(360n/365))x[\cos\Phi\cos\delta(\sin\omega_2-\sin\omega_2)$

$+\pi(\omega2-\omega1)x(1/180)\sin\Phi\sin\delta]$

=12x3600x1367x1/πx(1 +0.033cos(360x92/365)x

[Cos(-17.8˚)cos(4.41˚)(sin(0˚)-sin(-15˚))+
π((0)-(-15))x1/180xsin(-17.8˚)sin(4.41˚)]

4500955.80 J/m^2

4.500MJ/m^2

At 11:30 , G= 860W/m^2

I =860x3.6/1000 MJ/m^2

=3.096MJ/m^2

Applying equation (1.15) to get the hourly clearness index from 11:00 to 12:00

$K_T = \frac{I}{Io}$

= 3.096/4.5

0.688

Using Orgill and Hollard model to calculate the hourly clearness index

$$\frac{Id}{I} = \begin{cases} 1.0 - 0.249k_T & \text{for } 0 < k_T < 0.35 \\ 1.557-1.84k_T & \text{for } 0.35 < k_T < 0.75 \\ 0.177 & \text{for } k_T > 0.75 \end{cases}$$

$\frac{Id}{I}$ = 1.557-1.84x0.688

=0.29108

I_d = 0.29108x 3.096

= 0.9012MJ/m^2

To calculate the beam component equation (1.) is used.

$I_b = I – I_d$

= 3.096 – 0.9012

= 2.1948MJ/m^2

To calculate the beam component on a tilted plane there need to evaluate the geometric factor R_b.

$R_b = Cos\theta/Cos\theta_z$

$Cos\theta = Cos(\Phi+\beta)Cos\delta Cos\omega+Sin(\Phi+\beta)Sin\delta$

$= Cos(-17.8^\circ+37.5^\circ)Cos4.41^\circ Cos(-7.5^\circ)$

$= 0.9565729$

$\Theta = Cos^{-1}(0.9565729)$

$= 16.94^\circ$

$Cos\theta_z = Cos(-17.8^\circ)Cos(4.41^\circ)Cos(-7.5^\circ)+Sin(-17.8^\circ)Sin(4.41^\circ)$

$=0.917683$

$R_b = 0.9565729/0.917683$

= 1.042378

Radiation on a tilted plane applying the Liu and Jordan (1963) Isotropic model.

$\rho = 0.22$

Investigating the Impact of ground albedo on the performance of PV systems. Y Kotak and M.S.Gul (Heriot Watt University)

$I_T = I_bR_b + I_d(1+Cos\beta)/2+I_h\rho(1-Cos\beta)/2$

= 2.19x1.0423+0.9012(1+cos37.5)/2+3.096x0.22x(1-cos37.5)/2

= 3.161MJ/m^2

Applying the simplified Hottel and Woertz (1942) model:

$I_T = I_bR_b + I_d$

= 2.19x1.0423 +0.9012

3.18MJm^2

The simplified hotel and Woertz model is adopted in this study. The estimation for diffuse radiation is 0.6% lower in the Liu and Jordan isotropic model compared to the simplified Hottel and Woertz model.

Radiation income on the tilted plane on a pyranometric scale is got by converting I_T to the units of W/m^2.

$G_T = I_T x 10^6/3600$

=3.18x1000/3.6

= 883W/m^2.

The tank temperature T_s was read from the instruments every 15 minutes. At 11:30 it was 34.4˚C.

The tank temperature increase or decrease ΔT was calculated by subtracting the previous reading from the current reading. At 11:30 ΔT was 2.1˚C.

The ambient temperature was read from the instruments from T_4. At 11:30, Ta =T4=32˚C.

The shade cast on the collector was measured with a tape measure. It came as a rectangle, a triangle or both. The area of the shade was calculated separately.

To get the effective collector area at any incidence angle the shade area was subtracted from the collector area of 2.34m^2.

At 11:30 effective collector area A_C was 2.1879m^2

To calculate the incidence angle modifier K_θ, equation (3.11) was used.

K_θ =1-0.136((1/Cosθ)-1)

= 1-0.136((1/Cos16.94˚)/1)

= 0.9938

To calculate ΔT/I at 11:30

$(T_s-T_a)/(G_TK_\theta)$=(34.4˚-32˚)/(883x0.9938)

= 0.00269329˚Cm^2/W

To calculate the efficiency at 11:30

Applying equation (3:10) and adjusting for the incident angle modifier K_θ.

$\eta = Mcp\Delta T/(\Delta t x A_C x G_T x K_\theta)$

=150x4200x2.1/15x60x2.1879x883x0.9938

= 0.7656

The experiments were performed on 2, 22 and 30 April,2017. Another set of readings was also performed on 20 May, 2017.

Graphs of collector efficiency, η was plotted against $(T_s-T_a)/G_T$ with both η and G_T modified by the incident angle modifier to take into account the effect of the incidence angle on the optical response of the collector. See Tables 4.1, 4.2, 4.3 and 4.4

The second part of the characterisation process was to study the temperature response of the storage tank on its own in the absence of radiation. This was done by sliding back the collector frame into the trailer and continue taking reading every 30 minutes until midnight. See temperature decay Tables 4.5, 4.6 and 4.7.

Table 4.1 Data collected on 2 April, 2017

Time	ω°	δ	I_O(MJ/m^2)	G(W/m^2)	I(MJ/m^2)	K_T	I_b(MJ/m^2)	I_d(MJ/m^2)	R_b	I_T(MJ/m^2)	G_T(W/m^2)	T_s($^{\circ}$C)	ΔT($^{\circ}$C)	T_a($^{\circ}$C)	A_{shade}(m^2)	A_C(m^2)	θ°	K_θ	$(T_S-T_a)/(G_T*K_\theta)$	η/K_θ
11:00	-15	4.41	4.5	845	3.042	0.676	2.0893673	0.952633	1.042	3.129753	869.376	30.1	0	30.7	0.13923	2.20077	21.15	0.990177	-0.000683371	
11:15	-11.25	4.41	4.5	875	3.15	0.7	2.30265	0.84735	1.042	3.246711	901.8643	32.3	2.2	31.5	0.14859	2.19141	18.81	0.992326	0.000880244	0.785238
11:30	-7.5	4.41	4.5	860	3.096	0.688	2.1948163	0.901184	1.042	3.188182	885.6062	34.4	2.1	32	0.1521	2.1879	16.94	0.993831	0.00269329	0.763373
11:45	-3.75	4.41	4.5	875	3.15	0.7	2.30265	0.84735	1.042	3.246711	901.8643	36.5	2.1	32.7	0.17199	2.16801	15.72	0.994715	0.004191226	0.755816
12:00	0	4.41	4.5	960	3.456	0.768	2.9587507	0.497249	1.042	3.580268	994.5188	38.8	2.3	33.1	0.1872	2.1528	15.29	0.995009	0.00570281	0.755757
12:15	3.75	4.41	4.5	920	3.312	0.736	2.6404589	0.671541	1.042	3.422899	950.8054	40.9	2.1	33.6	0.19539	2.14461	15.72	0.994715	0.007637125	0.724734
12:30	7.5	4.41	4.5	930	3.348	0.744	2.7184421	0.629558	1.042	3.462175	961.7152	42.9	2	34.1	0.20826	2.13174	16.94	0.993831	0.00909387	0.687123
12:45	11.25	4.41	4.5	887	3.1932	0.7096	2.3906339	0.802566	1.042	3.293607	914.8907	44.7	1.8	34.6	0.21762	2.12238	18.81	0.992326	0.010954852	0.653919
13:00	15	4.41	4.186	850	3.06	0.731008	2.3983117	0.661688	1.046	3.170322	880.6451	46.8	2.1	34.5	0.21879	2.12121	21.15	0.990177	0.013829836	0.794731
13:15	18.75	4.41	4.186	760	2.736	0.653607	2.1443728	0.591627	1.046	2.834641	787.4003	48.4	1.6	34.9	0.23166	2.10834	23.82	0.987336	0.016927903	0.683308
13:30	22.5	4.41	4.186	800	2.88	0.688008	2.2572346	0.622765	1.046	2.983833	828.8424	49.9	1.5	35.1	0.26676	2.07324	26.73	0.983727	0.017565654	0.621145
13:45	26.25	4.41	4.186	788	2.8368	0.677688	2.223376	0.613424	1.046	2.939075	816.4098	51.4	1.5	34.8	0.26676	2.07324	29.79	0.979291	0.019911851	0.633461
14:00	30	4.41	3.57	710	2.556	0.715966	2.0032957	0.552704	1.056	2.668185	741.1624	52.7	1.3	34.7	0.27027	2.06973	32.98	0.973875	0.0236517	0.609132
14:15	33.75	4.41	3.57	726	2.6136	0.732101	2.0484404	0.56516	1.056	2.728313	757.8646	54	1.3	34.6	0.29718	2.04282	36.25	0.967358	0.024762661	0.607621
14:30	37.5	4.41	3.57	720	2.592	0.72605	2.0315111	0.560489	1.056	2.705765	751.6013	55.3	1.3	34.3	0.351	1.989	39.59	0.959519	0.026809293	0.634403
14:45	41.25	4.41	3.57	430	1.548	0.433613	1.2132636	0.334736	1.056	1.615943	448.873	56	0.7	34.3	0.3978	1.9422	42.97	0.950134	0.04593261	0.591553
15:00	45	4.41		300	1.08	0.7133	0.846463	0.233537	1.077	1.145178	318.1049	56.7	0.7	34.1	0.4329	1.9071	46.39	938825	66699.52224	
15:15	18:00	4.41		564	2.0304	0.7133	1.5913504	0.43905	1.077	2.152934	598.0372	57.3	0.6	33.9					0	

Table 4.2 Data collected on 22 April, 2017

Time	ω	δ	I_O(MJ/m²)	G(W/m²)	I(MJ/m²)	K_T	I_b	I_d	R_b	I_T	G_T	T_s	ΔT	T_a	A_{shade}	Ac	θ	K_θ	$(T_S-T_a)/(G_T*K_\theta)$	η/K_θ
9:00	-45	11.93	3.27	550	1.98	0.6055	1.1031	0.8769	1.1843	2.1833	606.47	24.2	0.3	22.1	0.033	2.307	43.86	0.9474	0.003280	
9:15	-41.25	11.93	3.27	563	2.0268	0.6198	1.1826	0.8442	1.1843	2.2447	623.54	25.3	1.1	23.3	0.0216	2.3184	40.34	0.9576	0.003350	
9:30	-37.5	11.93	3.27	580	2.088	0.6385	1.2902	0.7978	1.1843	2.3258	646.05	26.7	1.4	24	0.0137	2.3263	36.82	0.9661	0.004326	0.6749
9:45	-33.75	11.93	3.27	646	2.3256	0.7112	1.7479	0.5777	1.1843	2.6477	735.48	28.4	1.7	24.8	0.0079	2.3321	33.32	0.9732	0.005029	0.7129
10:00	-30	11.93	3.86	679	2.4444	0.6333	1.4867	0.9577	1.1546	2.6742	742.85	30.2	1.8	25.5	0.0028	2.3372	29.84	0.9792	0.006461	0.7411
10:15	-26.25	11.93	3.86	708	2.5488	0.6603	1.6770	0.8718	1.1546	2.8081	780.02	32.2	2	26.4	0.0012	2.3388	26.38	0.9842	0.007555	0.7797
10:30	-22.5	11.93	3.86	730	2.628	0.6808	1.8284	0.7996	1.1546	2.9107	808.52	34.2	2	26.8	0	2.34	22.97	0.9883	0.009261	0.7488
10:45	-18.75	11.93	3.86	759	2.7324	0.7079	2.0370	0.6954	1.1546	3.0473	846.48	36.2	2	27.8	0.011	2.329	19.62	0.9916	0.010007	0.7161
11:00	-15	11.93	4.17	790	2.844	0.6820	1.9848	0.8592	1.1423	3.1264	868.46	38.4	2.2	28.4	0.023	2.317	16.37	0.9943	0.011581	0.7697
11:15	-11.25	11.93	4.17	753	2.7108	0.6501	1.7326	0.9782	1.1423	2.9573	821.48	40.3	1.9	28.9	0.039	2.301	13.31	0.9962	0.013930	0.7063
11:30	-7.5	11.93	4.17	760	2.736	0.6561	1.7791	0.9569	1.1423	2.9892	830.32	42.3	2	29.4	0.044	2.296	10.59	0.9976	0.015573	0.7361
11:45	-3.75	11.93	4.17	780	2.808	0.6734	1.9151	0.8929	1.1423	3.0805	855.70	44.1	1.8	29.5	0.058	2.282	8.56	0.9985	0.017036	0.6462
12:00	0	11.93	4.17	804	2.8944	0.6941	2.0844	0.8100	1.1423	3.1910	886.39	46	1.9	30.1	0.069	2.271	7.77	0.9987	0.017961	0.6615
12:15	3.75	11.93	4.17	800	2.88	0.6906	2.0557	0.8243	1.1423	3.1725	881.26	48	2	30.4	0.077	2.263	8.56	0.9985	0.020002	0.7031
12:30	7.5	11.93	4.17	818	2.9448	0.7062	2.1862	0.7586	1.1423	3.2559	904.41	50	2	31	0.085	2.255	10.59	0.9976	0.021058	0.6881
12:45	11.25	11.93	4.17	748	2.6928	0.6458	1.6997	0.9931	1.1423	2.9347	815.18	51.6	1.6	30.2	0.093	2.247	13.31	0.9962	0.026351	0.6138
13:00	15	11.93	3.86	720	2.592	0.6715	1.7588	0.8332	1.1546	2.8639	795.53	53.1	1.5	31	0.099	2.241	16.37	0.9943	0.027941	0.5924
13:15	18.75	11.93	3.86	600	2.16	0.5596	1.0209	1.1391	1.1546	2.3178	643.84	54.3	1.2	31.9	0.105	2.235	19.62	0.9916	0.035085	0.5887
13:30	22.5	11.93	3.86	522	1.8792	0.4868	0.6366	1.2426	1.1546	1.9776	549.34	55.2	0.9	30.7	0.117	2.223	22.97	0.9883	0.045127	0.5220
13:45	26.25	11.93	3.86	420	1.512	0.3917	0.2476	1.2644	1.1546	1.5503	430.63	55.9	0.7	30.2	0.138	2.202	26.38	0.9842	0.060638	0.5250
14:00	30	11.93	2.27	360	1.296	0.5709	0.6396	0.6564	1.1843	1.4139	392.74	56.5	0.6	29.6	0.129	2.211	29.84	0.9792	0.069947	0.4939
14:15	33.75	11.93	2.27	350	1.26	0.5551	1.0370	0.2230	1.1843	1.4511	403.09	57	0.5	28.8	0.174	2.166	33.32	0.9732	0.068088	0.4119
14:30	37.5	11.93	2.27	420	1.512	0.6661	1.2444	0.2676	1.1843	1.7413	483.71	57.7	0.7	29.1	0.188	2.152	36.82	0.9661	0.057123	0.4872
14:45	41.25	11.93	2.27	484	1.7424	0.7676	1.4340	0.3084	1.1843	2.0067	557.41	58.5	0.8	29.1	0.209	2.131	40.34	0.9576	0.055081	0.4923
15:00	45	11.93	2.646	320	1.152	0.4354	0.9481	0.2039	1.251	1.3900	386.10	59	0.5	29	0.24	2.1	43.86	0.9474	0.082015	0.4556

Table 4.3 Data collected on 30 April 2017

Time	ω^*	δ	I_O(MJ/m^2)	G(W/m^2)	I(MJ/m^2)	K_T	I_b	I_d	R_b	I_T	G_T	T_s	ΔT	T_a	A_{shade}	Ac	θ	K_θ	$(T_S-T_a)/G_T$	η
9:00	-45	14.59	3.49	706	2.5416	0.728	1.990	0.552	1.235	3.01	836	27	0	22.1	0.0238	2.3162	43.18	0.9494	0.0061	
9:15	-41.25	14.59	3.49	713	2.5668	0.735	2.044	0.523	1.235	3.05	846	27.7	0.7	23.8	0.0158	2.3242	39.65	0.9594	0.0048	
9:30	-37.5	14.59	3.49	680	2.448	0.701	1.796	0.652	1.235	2.87	797	29.5	1.8	25.2	0.00975	2.33025	36.12	0.9676	0.0055	0.700948
9:45	-33.75	14.59	3.49	705	2.538	0.727	1.982	0.556	1.235	3.00	834	31.5	2	26.4	0.0047	2.3353	32.6	0.9745	0.0062	0.737269
10:00	-30	14.59	4.074	730	2.628	0.645	1.655	0.973	1.197	2.95	821	33.4	1.9	27.2	0.0005	2.3395	29.08	0.9804	0.0077	0.706642
10:15	-26.25	14.59	4.074	720	2.592	0.636	1.591	1.001	1.197	2.91	807	35.2	1.8	28.2	0	2.34	25.57	0.9852	0.0088	0.677227
10:30	-22.5	14.59	4.074	740	2.664	0.754	1.721	0.943	1.197	3.00	834	37.2	2	28.6	0	2.34	22.08	0.9892	0.0104	0.725033
10:45	-18.75	14.59	4.074	710	2.556	0.627	1.527	1.029	1.197	2.86	794	39.1	1.9	29.1	0	2.34	18.62	0.9925	0.0126	0.721649
11:00	-15	14.59	4.37	600	2.16	0.494	1.778	0.382	1.181	2.48	689	40.6	1.5	29.2	0	2.34	15.2	0.995	0.0166	0.654174
11:15	-11.25	14.59	4.37	640	2.304	0.527	0.952	1.352	1.181	2.48	688	42.2	1.6	29.4	0.0583	2.2817	11.9	0.997	0.0186	0.715761
11:30	-7.5	14.59	4.37	873	3.1428	0.719	2.408	0.735	1.181	3.58	994	44.4	2.2	30.2	0.0174	2.3226	8.8	0.9983	0.0143	0.668133
11:45	-3.75	14.59	4.37	850	3.06	0.700	2.518	0.542	1.181	3.52	977	46.5	2.1	31	0.0233	2.3167	6.24	0.9992	0.0158	0.650235
12:00	0	14.59	4.37	790	2.844	0.651	2.341	0.503	1.181	3.27	908	48.5	2	31.6	0.0291	2.3109	5.11	0.9995	0.0186	0.667776
12:15	3.75	14.59	4.37	720	2.592	0.593	1.385	1.207	1.181	2.84	790	50.3	1.8	31.6	0.0408	2.2992	6.24	0.9992	0.0237	0.694565
12:30	7.5	14.59	4.37	680	2.448	0.560	2.015	0.433	1.181	2.81	781	51.9	1.6	31.7	0.0466	2.2934	8.8	0.9983	0.0258	0.626127
12:45	11.25	14.59	4.37	550	1.98	0.453	1.630	0.350	1.181	2.27	632	53.2	1.3	31.5	0.0524	2.2876	11.9	0.997	0.0344	0.63139
13:00	15.	14.59	4.074						1.197			54.2		30.7			15.2	0.995		
13:15	18.75	14.59	4.074						1.197			54.2		29.3			18.62	0.9925		
13:30	22.5	14.59	4.074						1.197			54.5		29.3			22.08	0.9892		
13:45	26.25	14.59	4.074						1.197			55.2		27.9			25.57	0.9852		
14:00	30	14.59	3.49	700	2.52	0.722	1.944	0.576	1.235	2.98	827	55.2	0	27.7			29.08	0.9804		
14:15	33.75	14.59	3.49	600	2.16	0.619	1.257	0.903	1.235	2.46	682	55.2	0	27.7			32.6	0.9745		
14:30	37.5	14.59	3.49	340	1.224	0.351	0.108	1.116	1.235	1.25	347	55.6	0.4	28.1	0.1521	2.1879	36.12	0.9676	0.0818	0.381096
14:45	41.25	14.59	3.49	500	1.8	0.516	0.706	1.094	1.235	1.97	546	56.5	0.9	28	0.1505	2.1895	39.65	0.9594	0.0544	0.549232
15:00	45	14.59	2.67	450	1.62	0.607	1.333	0.287	1.322	2.05	569	57.4	0.9	29.6	0.1739	2.1661	43.18	0.9494	0.05143	0.538155

Table 4.4 Data collected on 20 May 2017

Time		δ	I_O(MJ/m²)	G(W/m²)	I(MJ/m²)	K_T	I_b	I_d	R_b	I_T	G_T	T_s	ΔT	T_a	A_{shade}	Ac	θ	K_θ	$(T_S-T_a)/G_T$	η
8:00		19.92	2.1075	300	1.08	0.5125	0.4168	0.6632	1.4827	1.28	356	24	0	14.2	0.056	2.284	56.12	0.8920	0.0246	
8:15		19.92	2.1075	350	1.26	0.5979	0.6843	0.5757	1.4827	1.59	442	24.9	0.9	16.6	0.0441	2.2959	52.65	0.9118	0.0171	0.6812
8:30		19.92	2.1075	394	1.4184	0.6730	0.9664	0.4520	1.4827	1.88	524	26	1.1	18.7	0.0345	2.3055	49.17	0.9280	0.0129	0.6874
8:45		19.92	2.1075	440	1.584	0.7516	1.3036	0.2804	1.4827	2.21	615	27.3	1.3	20.5	0.0256	2.3144	45.69	0.9413	0.0104	0.6794
9:00		19.92	2.8993	480	1.728	0.5960	0.9325	0.7955	1.3482	2.05	570	28.6	1.3	21.6	0.0156	2.3244	42.2	0.9524	0.0117	0.7209
9:15		19.92	2.8993	519	1.8684	0.6444	1.1748	0.6936	1.3482	2.28	633	30.2	1.6	22.7	0.00845	2.33155	38.71	0.9617	0.0114	
9:30		19.92	2.8993	556	2.0016	0.6904	1.4277	0.5739	1.3482	2.50	694	32	1.8	23.6	0.0027	2.3373	35.2	0.9696	0.0117	
9:45		19.92	2.8993	596	2.1456	0.7400	1.7265	0.4191	1.3482	2.75	763	33.6	1.6	24.4	0.00045	2.33955	31.7	0.9762	0.0118	0.6428
10:00		19.92	3.4587	629	2.2644	0.6547	1.4665	0.7979	1.3061	2.71	754	35.6	2	25.1	0	2.34	28.19	0.9817	0.0137	
10:15		19.92	3.4587	665	2.394	0.6922	1.7155	0.6785	1.3061	2.92	811	37.5	1.9	25.6	0	2.34	24.67	0.9863	0.0145	0.7107
10:30		19.92	3.4587	687	2.4732	0.7151	1.8765	0.5967	1.3061	3.05	847	39.5	2	26.4	0	2.34	21.15	0.9902	0.0153	0.7137
10:45		19.92	3.4587	712	2.5632	0.7411	2.0675	0.4957	1.3061	3.20	888	41.4	1.9	27.1	0	2.34	17.63	0.9933	0.0160	0.6445
11:00		19.92	3.7482	727	2.6172	0.6983	1.9048	0.7124	1.2669	3.13	868	43.5	2.1	28	0	2.34	14.1	0.9958	0.0178	0.7266
11:15		19.92	3.7482	738	2.6568	0.7088	1.9852	0.6716	1.2669	3.19	885	45.4	1.9	28.9	0	2.34	10.58	0.9976	0.0186	0.6436
11:30		19.92	3.7482	746	2.6856	0.7165	2.0447	0.6409	1.2669	3.23	898	47.6	2.2	29.6	0	2.34	7.06	0.9990	0.0200	
11:45		19.92	3.7482	745	2.682	0.7155	2.0372	0.6448	1.2669	3.23	896	49.5	1.9	30.1	0	2.34	3.53	0.9997	0.0216	0.6345
12:00		19.92	3.7482	756	2.7216	0.7261	2.1202	0.6014	1.2669	3.29	913	51.6	2.1	30.6	0	2.34	0.22	1.0000	0.0230	0.6879
12:15		19.92	3.7482	749	2.6964	0.7194	2.0672	0.6292	1.2669	3.25	902	53.4	1.8	31.1	0	2.34	3.53	0.9997	0.0247	0.5969
12:30		19.92	3.7482	742	2.6712	0.7127	2.0149	0.6563	1.2669	3.21	891	55.3	1.9	31.4	0	2.34	7.06	0.9990	0.0268	0.6383
12:45		19.92	3.7482	727	2.6172	0.6983	1.9048	0.7124	1.2669	3.13	868	57	1.7	31.4	0	2.34	10.58	0.9976	0.0294	0.5871
13:00		19.92	3.4587	709	2.5524	0.7380	2.0441	0.5083	1.3061	3.18	883	58.7	1.7	31.4	0	2.34	14.1	0.9958	0.0308	0.5785
13:15		19.92	3.4587	692	2.4912	0.7203	1.9140	0.5772	1.3061	3.08	855	60.4	1.7	31.6	0	2.34	17.63	0.9933	0.0335	0.5990
13:30		19.92	3.4587	673	2.4228	0.7005	1.7733	0.6495	1.3061	2.97	824	61.5	1.1	31.6	0	2.34	21.15	0.9902	0.0359	

13:45		19.92	3.4587	641	2.3076	0.6672	1.5475	0.7601	1.3061	2.78	773	63.3	1.8	31.4	0.0022	2.3378	24.67	0.9863	0.0407	
14:00		19.92	3.4587	619	2.2284	0.6443	1.4005	0.8279	1.3482	2.72	754	64.5	1.2	31.4	0.0115	2.3285	28.19	0.9817	0.0431	0.4871
14:15		19.92	2.8993	572	2.0592	0.7102	1.5441	0.5151	1.3482	2.60	721	65.7	1.2	31.2	0.024	2.316	31.7	0.9762	0.0467	0.5151
14:30		19.92	2.8993	550	1.98	0.6829	1.3852	0.5948	1.3482	2.46	685	66.4	0.7	31	0.0451	2.2949	35.2	0.9696	0.0502	
14:45		19.92	2.8993	460	1.656	0.5712	0.8180	0.8380	1.3482	1.94	539	67.2	0.8	31	0.0707	2.2693	38.71	0.9617	0.0646	0.4760
15:00		19.92	2.8993	440	1.584	0.5463	0.7100	0.8740	1.4827	1.93	535	67.9	0.7	30.8	0.0972	2.2428	42.2	0.9524	0.0660	0.4286
15:15		19.92	2.1075	431	1.5516	0.7362	1.2376	0.3140	1.4827	2.15	597	68.4	0.5	30.4	0.129	2.211	45.69	0.9413	0.0599	
15:30		19.92	2.1075	392	1.4112	0.6696	0.9527	0.4585	1.4827	1.87	520	68.7	0.3	30.1	0.1728	2.1672	49.17	0.9280	0.0689	
15:45		19.92	2.1075	345	1.242	0.5893	0.6550	0.5870	1.4827	1.56	433	68.9	0.2	29.9	0.2074	2.1326	52.65	0.9118	0.0822	
16:00		19.92	2.1075	327	1.1772	0.5586	0.5542	0.6230	1.9022	1.68	566	69	0.1	29.7	0.261	2.079	56.12	0.8920	0.0752	
16:15		19.92	1.1397	264	0.9504	0.8339	0.7822	0.1682	1.9022	1.66	460	69	0	29.1	0.351	1.989	59.58	0.8674	0.0752	
16:30		19.92	1.1397	222	0.7992	0.7012	0.5860	0.2132	1.9022	1.33	369	68.5	-0.5	28.4	0.4274	1.9126	63.02	0.8362	0.0909	

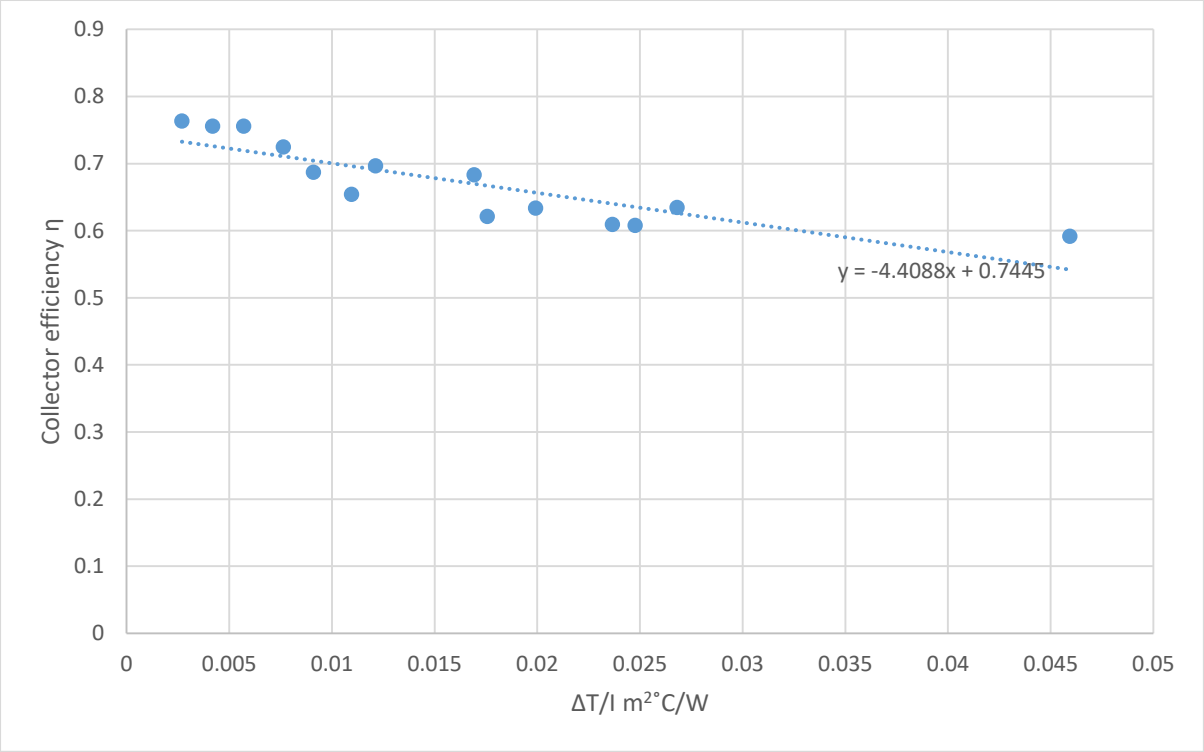

Fig.4.1 graph of η vs $\Delta T/G_t$, 2017developed on 2 April

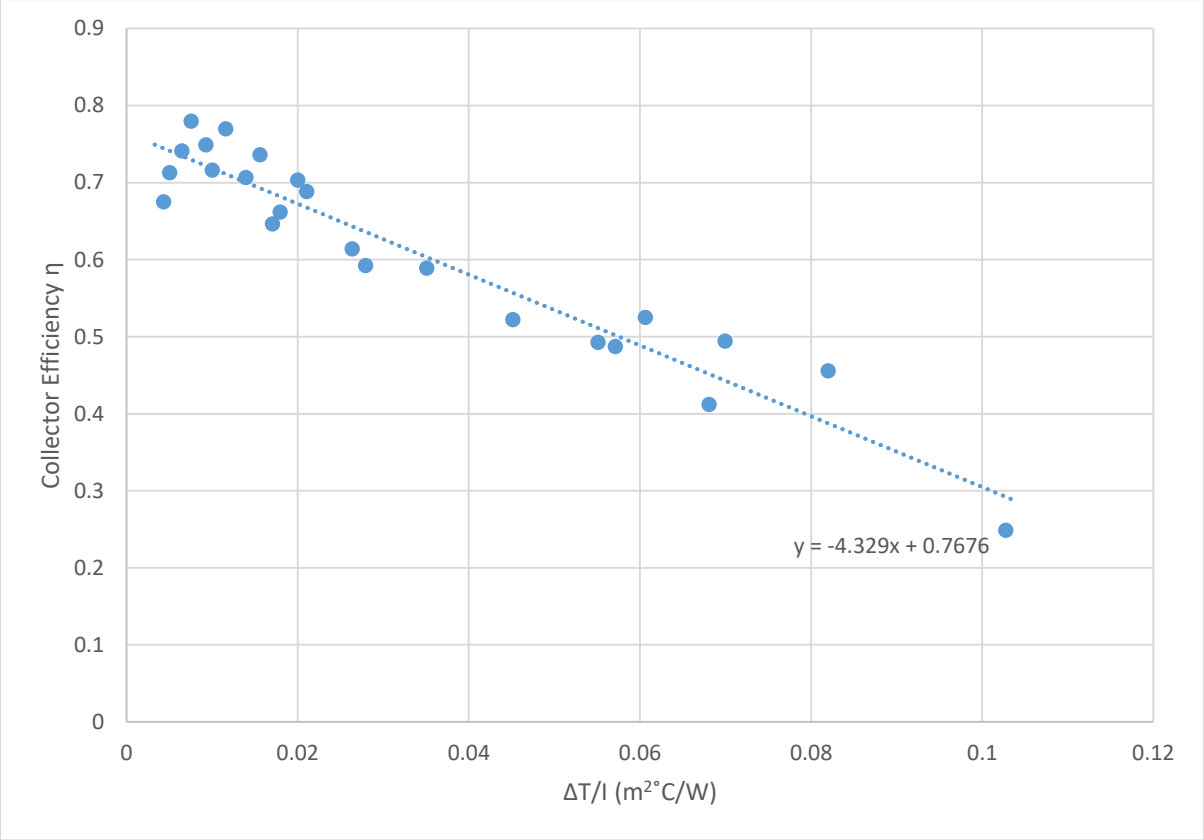

Fig.4.2 graph of η vs $\Delta T/G_t$ developed on 22 April 2017

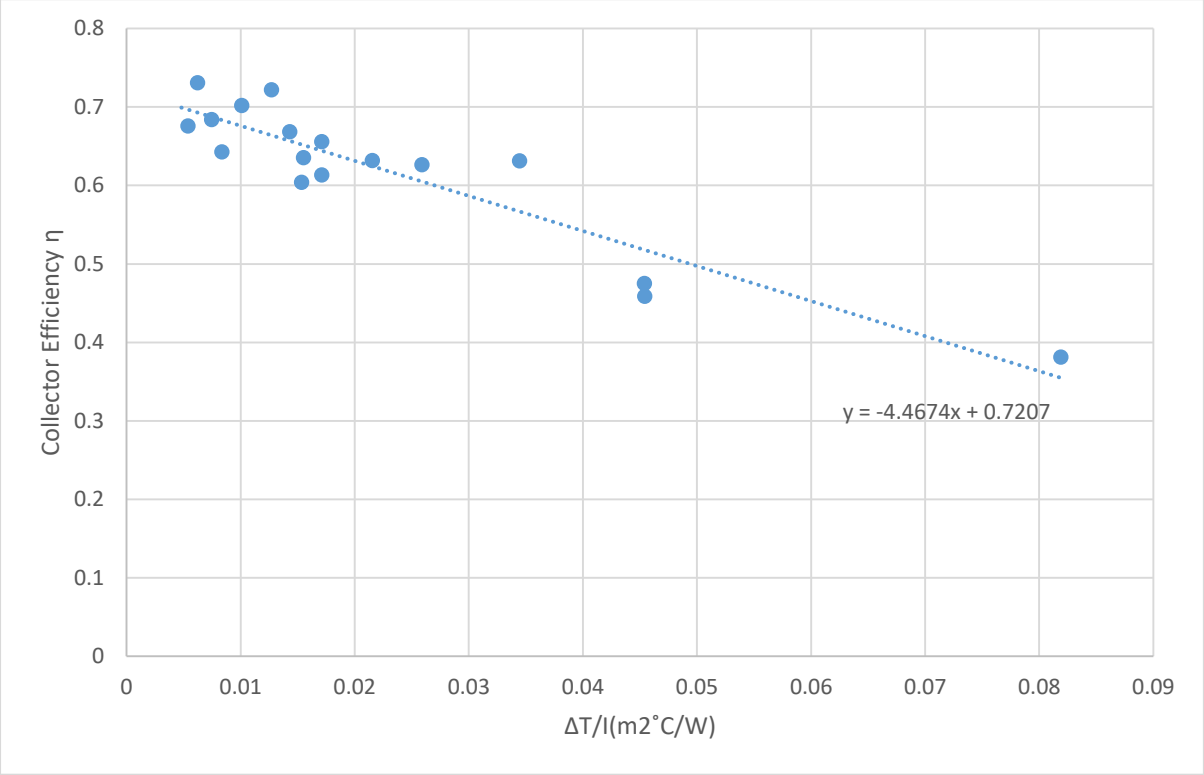

Fig.4.3 graph of η vs ΔT/Gt developed on 30 April 2017

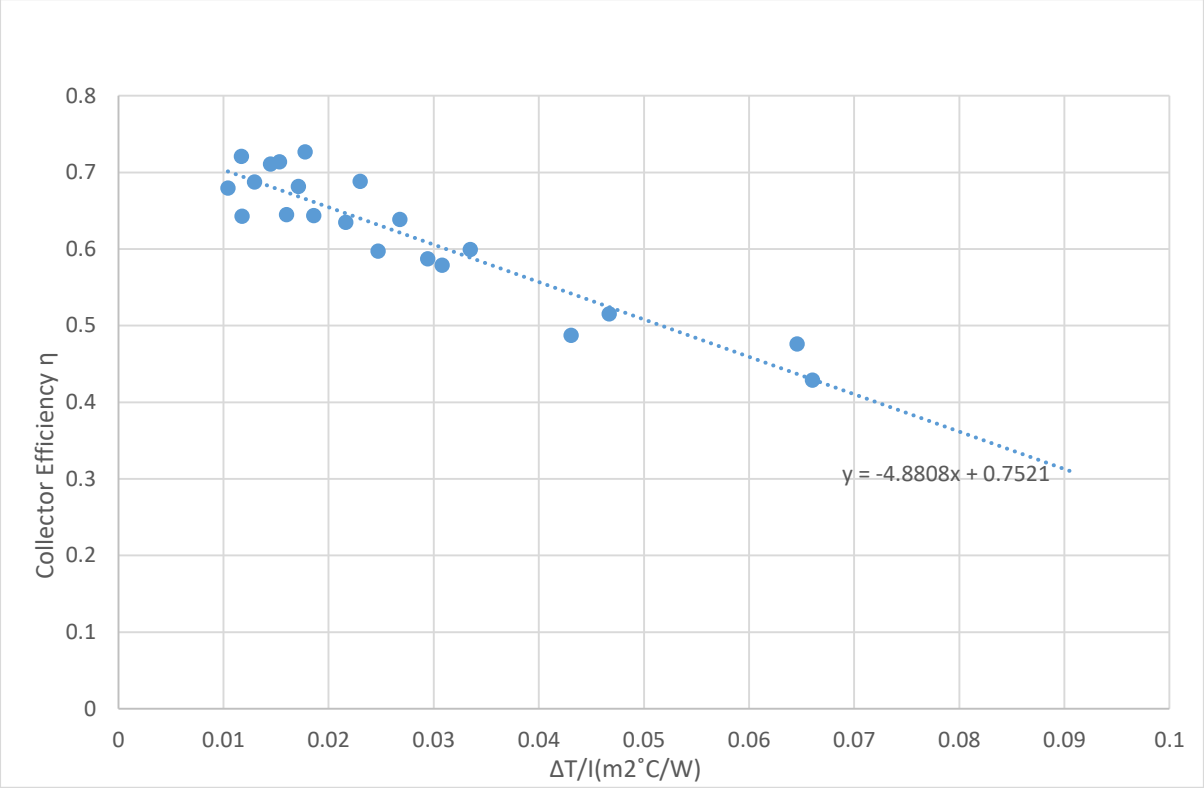

Fig.4.4 graph of η vs ΔT/Gt developed on 20 May 2017

Storage tank characterisation

Table 4.5

Measurements of tank temperatures on 2 April 2017

Time	Tst	Ta
15:30	57.5	34.3
16:00	57.5	33.8
16:30	57.4	31.9
17:00	57.3	30.1
17:30	57.3	28.2
18:00	57.1	26.5
18:30	57	25.1
19:00	56.9	23.9
19:30	56.7	23
20:00	56.6	22.2
20:30	56.4	21.5
21:00	56.3	21
21:30	56.1	20.4
22:00	55.9	20.1
22:30	55.8	19.7
23:00	55.6	19.2
23:30	55.4	18.7
0:00	55.3	18.2

Table 4.6

22 April 2017

Time	Tst	Ta
16:30	59.5	26.7
17:00	59.4	26.6
17:30	59.2	26.5
18:00	59.1	25.4
18:30	59	24.2
19:00	58.8	23.4
19:30	58.7	22.7
20:00	58.5	22.2
20:30	58.4	21.9
21:00	58.2	21.6
21:30	58	21.3
22:00	57.9	21.1
22:30	57.7	20.9
23:00	57.6	20
23:30	57.4	19.4
24:00:00	57.2	18.9

Table 4.7

30 April 2017

Time	Tst	Ta
17:00	58.4	26.4
17:30	58.3	25.1
18:00	58.1	24.2
18:30	58	23.3
19:00	57.8	22.8
19:30	57.7	22
20:00	57.5	21
20:30	57.4	20.6
21:00	57.2	19.9
21:30	57	19.2
22:00	56.9	18.6
22:30	56.7	18.2
23:00	56.5	17.8
23:30	56.4	17.4
24:00:00	56.2	17

To calculate UA_s applying equation (2.40)

$UA_s = Mcp[\ln(T_{s\ av\ beg} - T_{a\ av\ beg}) - \ln(T_{s\ end} - T_{a\ end})]/(t_{end} - t_{beg})$

For 2 April, 2017

UAs = 1.61 W/˚C

For 22 April, 2017

UAs = 1.53W/˚C

For 30 April, 2017

UAs = 1.75W/˚C

Average UAs = 1.63 W/˚C

CHAPTER 5

5.1 Results

After averaging the results from the four graphs the following parameters were obtained:

$F_R(\tau\alpha) = 0.7556$

$F_R U_L = 4.47\ W/m^2{}^\circ C$

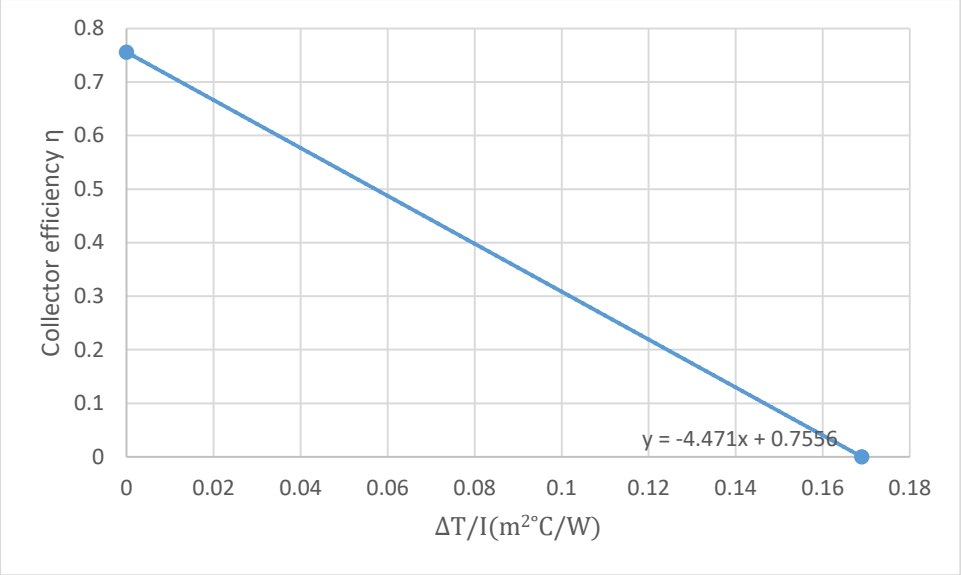

Fig.5.1

Graph of η vs $\Delta T/G_t$ showing the averaged parameters that define the model.

From analysis of the results of observing the temperature decay of the storage tank at zero insolation the value of UsAs was determined.

$UsA_S = 1.63$ W/˚C

Surface area of storage tank, As was determined from dimensions.

As = 2.41 m^2

Hence Us = 0.68 W/m^2˚C

5.2 Validation

This data was tested on two clear days by predicting the tank temperatures and measuring the tank temperatures at the indicated times of the day.

On 20 May 2017 the measurements were done from 08:00 hours to 16:30 hours.

On 25 May 2017 the measurements were performed from 08:00 hours to 06:00 hours the following morning. An Excel based thermo-economic computing model designed by Engineer T. Hove[1] was used to perform the calculations for predicting storage temperatures on a clear day. The computing model is based on the equation 3.6 dealt with in Chapter 3.

The data is tabled in Table (5.1) and Table (5.2)

The graphs are shown in Fig.(5.2) and Fig.(5.3)

[1] Engineer T. Hove is a Senior Lecturer in the Dept. of Mechanical Engineering University of Zimbabwe.

Table 5.1

Time	Measured ˚C	Predicted ˚C
8:00	24	24
9:00	28.6	28
10:00	35.6	34
11:00	43.5	41
12:00	51.6	50
13:00	58.7	58
14:00	64.5	64
15:00	67.9	68
16:00	69	69
17:00	68	68

Table comparing measured tank temperatures versus temperatures predicted by the model.

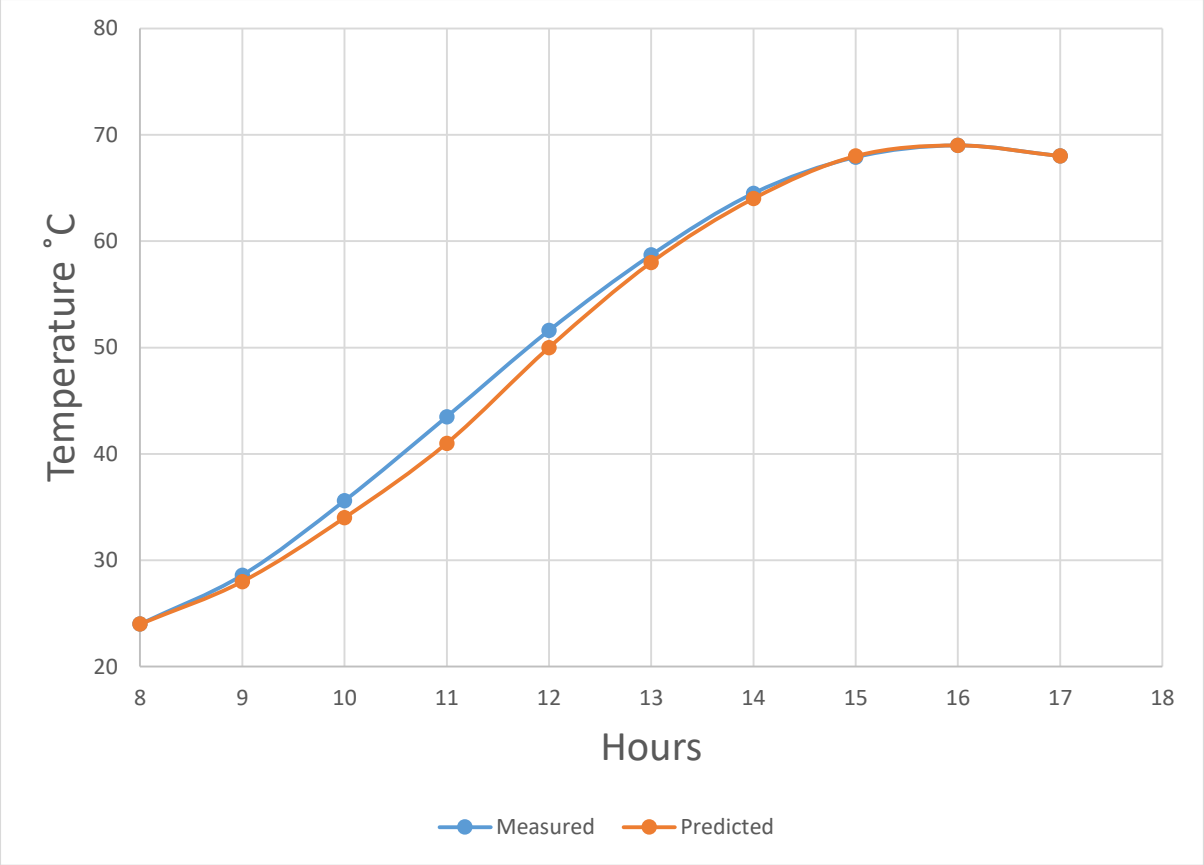

Fig.5.2 graph comparing measured tank temperatures versus temperatures predicted by the model during day only.

Table 5.2

Data taken on 25 May 2017

Hour	Measured˚C	Predicted˚C
1	38.6	39
2	42.7	41
3	48.9	47
4	56	54
5	63.4	61
6	69.8	68
7	74.8	74
8	77.6	78
9	78.3	78
10	78	78
11	77.5	77
12	77.1	77
13	76.6	76
14	76.1	75
15	75.5	75
16	75	74
17	74.5	73
18	73.5	73
19	73	72
20	72.3	71
21	71.8	71
22	71.3	70

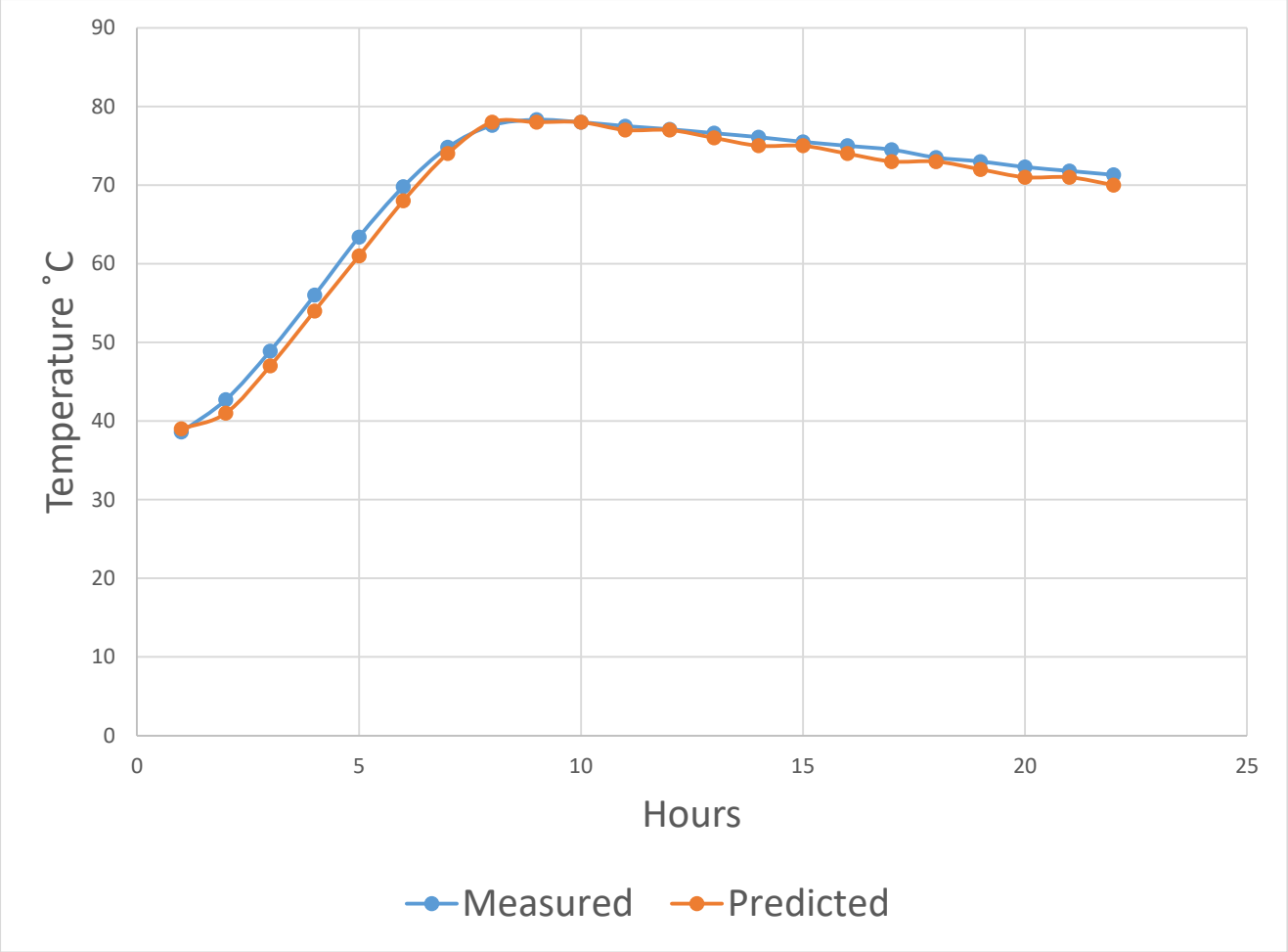

Fig.5.3

Data taken on 25 May round the clock to validate results during day and night.

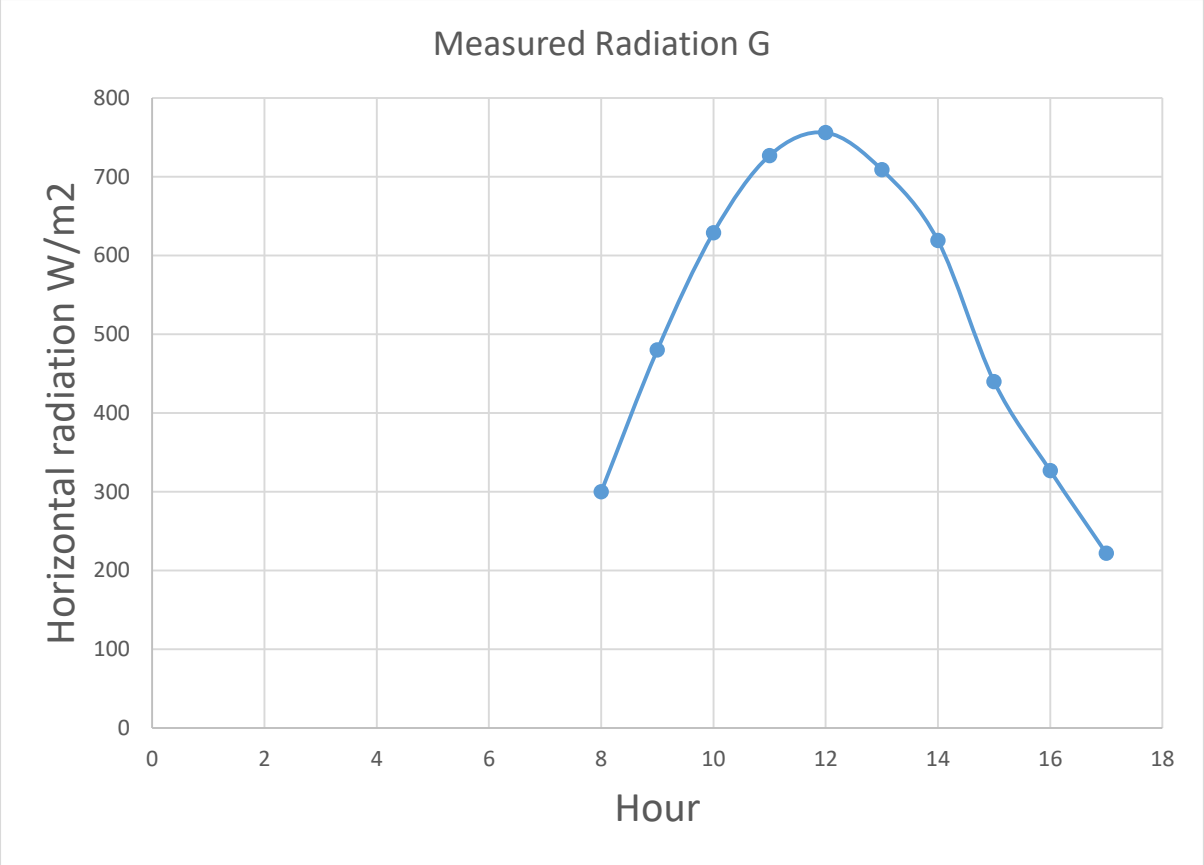

Fig.5.4

Measured horizontal radiation on 20 May 2017

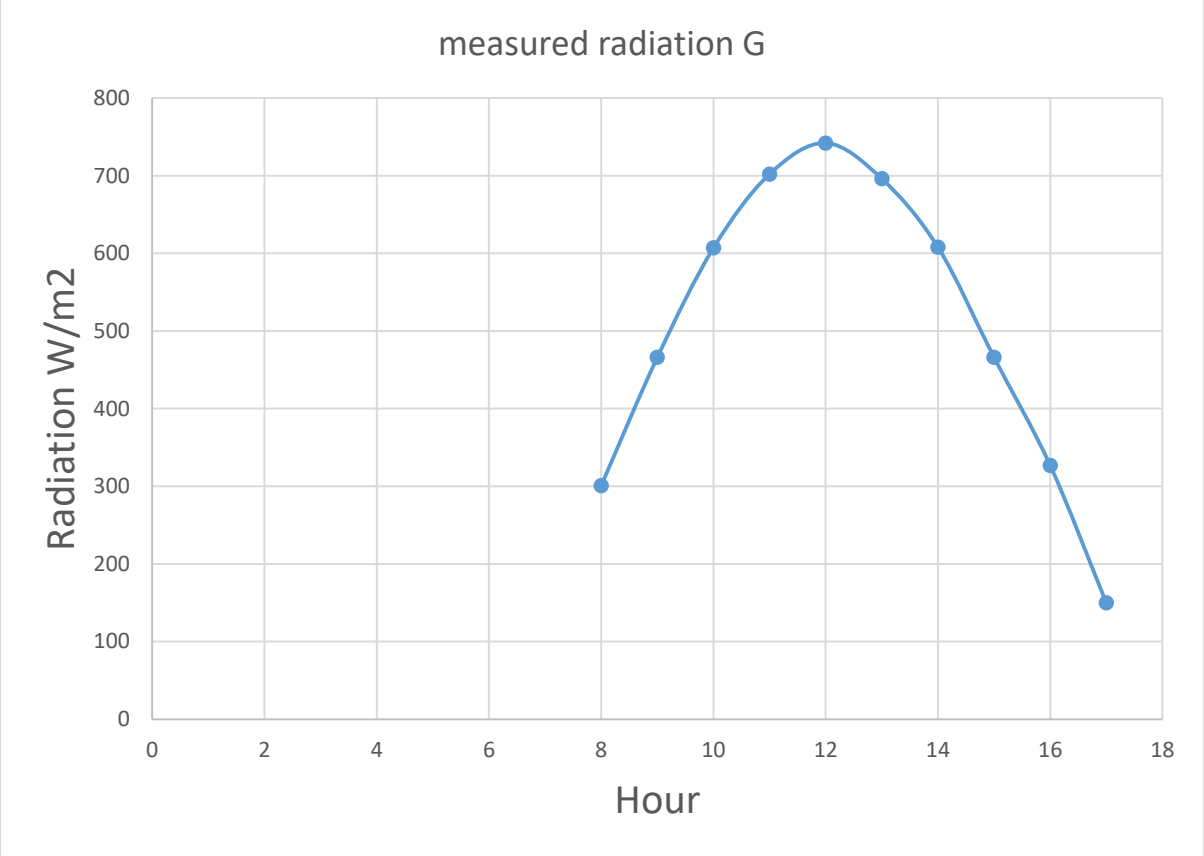

Fig.5.5

Measured horizontal radiation on 25 May 2017

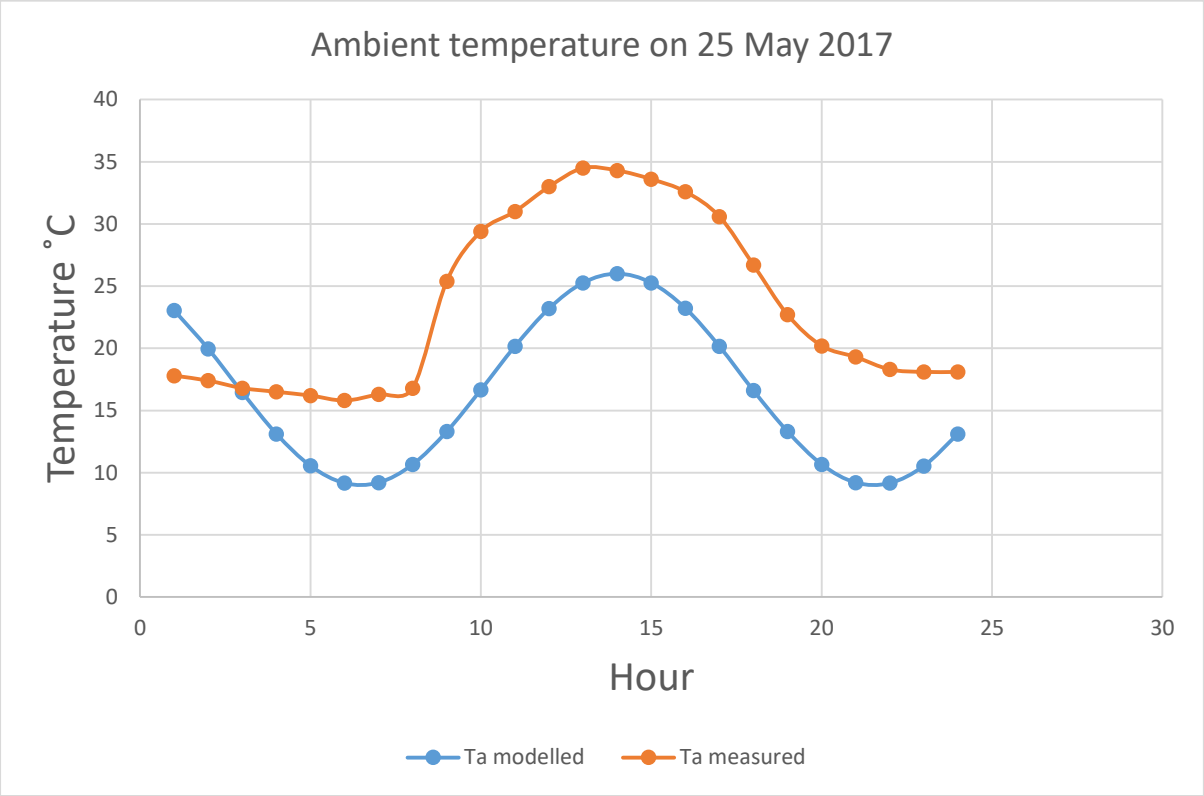
Ambient temperature on 25 May 2017
Temperature °C
40
35
30
25
20
15
10
5
0
0
5
10
15
20
25
30
Hour
Ta modelled
Ta measured

Fig.5.6

CHAPTER 6

Discussion of Results

The prediction of the storage tank temperatures to an accuracy of 1.1˚C using this model is an indication that this method of characterisation of SWH systems is a credible method and the model can be used to characterise SWHS.

The experiment was performed at an average collector efficiency of 48 % see Table 6.1 and total daily irradiation of 6.9 kWh/day m^2.

At lower temperatures the difference between the predicted and the measured temperature is higher than at higher temperatures. The assumption that the tank temperature is homogeneous is in fact not accurate as there is always a degree of stratification even with horizontal tanks. Davidson J.A. et al (1994)went further to define a non-dimensional parameter the Mix number based on the height weighted energy or moment of energy to derive a range from 0 to 1 with 0 representing a perfectly stratified mix or 0 mix and 1 a fully mixed tank. The importance of stratification is that it is the water at lower temperatures that is fed back into the collector at inlet fluid temperature. In the efficiency equation when Ts is low and Ta is constant it means the heat loss is reduced hence the efficiency of

heat removal and consequently heat gain is increased. This is consistent with the observation that at lower temperatures the measured temperatures are higher than the predicted ones.

The assumption that F_R is constant is then challenged at lower temperatures and this is one of the tacit assumptions of the Hottel-Whillier-Bliss equation. The assumption in this model that heat transfer is more prominent than mass transfer further gives rise to this anomaly. Experiments have shown that F_R increases with flow rate. IEA report (1993). The fact that this study works on the assumption of no mass flow but energy flow will of necessity understate the value of F_R. The understated value of the heat removal factor will result in the understatement of the useful energy gain and hence an understated value of the predicted tank storage temperature..

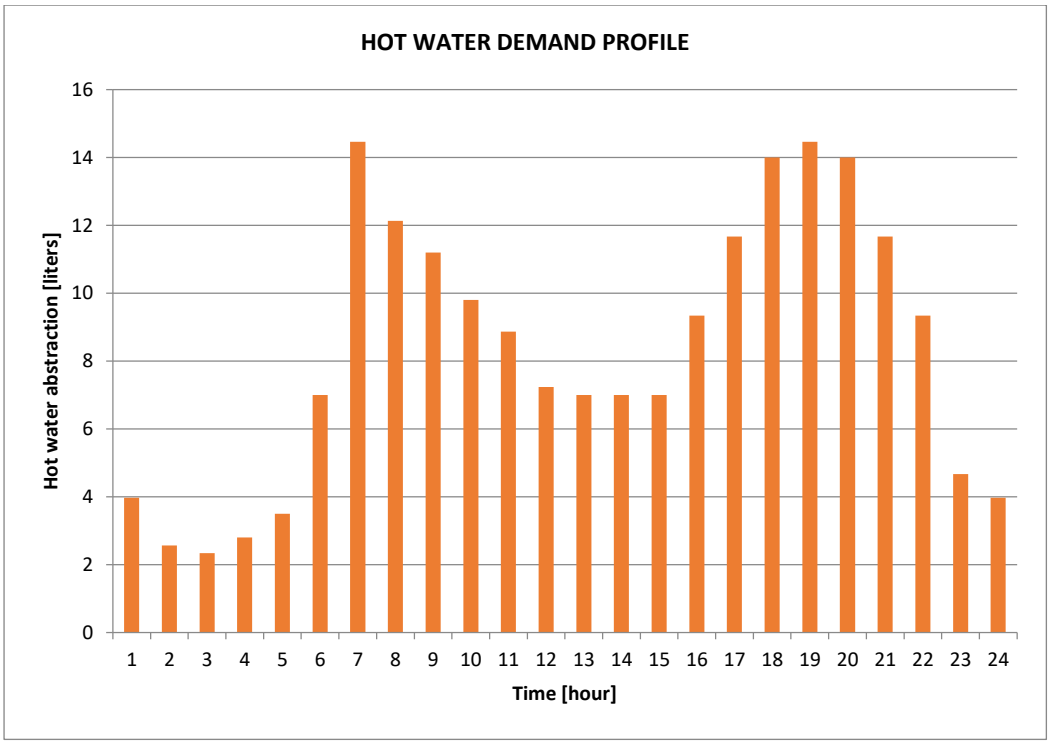

Fig.6.1 Domestic hot water temperature demand profile- Meyer (2000) assumptions for residential hot water consumption for residential accommodation.

When the demand is raised to 150 litres per day the temperature profile of the storage tank is as below:

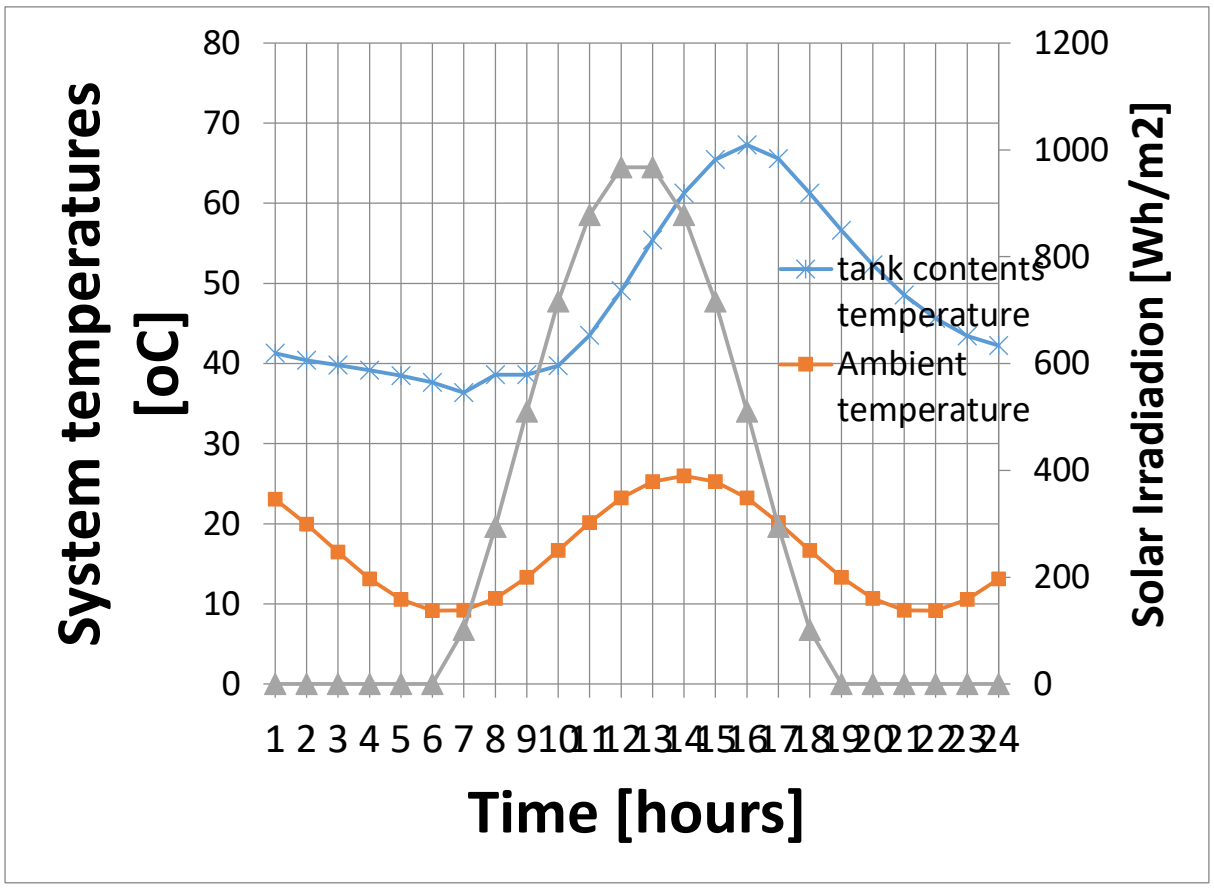

Fig.6.2

Thermal Energy Outputs

Total incident irradiation/m^2	6.9 kWh/day m^2
Collector Area/m^3 DHWD	15.60 m2/m^3
Storage, Vstorage/DHWD	0.87
Collector output	8 kWh/day
Collector output Energy/m^2	3.35 kWh/day m^2
Daily Collector Efficiency	48%
Storage Losses	0 kWh/day
other losses	0 kWh/day
Daily Energy Demand	6 kWh/day
Energy met by Solar	5 kWh/day
Solar Fraction	0.9

Table 6.1

The thermal parameters at 200 litres per day are as follows:

Total incident irradiation/m^2	6.9 kWh/day m^2
Collector Area/m^3 DHWD	11.70 m2/m^3
Storage, Vstorage/DHWD	91
Collector output	8 kWh/day
Collector output Energy/m^2	3.`40 kWh/day m^2
Daily Collector Efficiency	49%
Storage Losses	0 kWh/day
Other losses	0 kWh/day
Daily Energy Demand	8 kWh/day
Energy met by Solar	7 kWh/day
Solar Fraction	0.85

Table 6.2

It is possible given the solar water heating performance parameters to predict the thermal performance for the whole year in Harare if meteorological and environmental parameters are known. For the solar trailer the tilt and azimuth will be kept constant. The fixing of the tilt angle is in itself a disadvantage because the tilt angle is not optimised. For solar water heating optimum tilt angle is latitude + 5˚Kalogirou (2009)

The table below shows monthly mean daily solar radiation for Harare throughout the year in MJ/m^2 day. P.C. Jain - International Centre for theoretical Physics Trieste Italy. (1968-78) and the maximum and minimum temperatures throughout the year.

Day of Month	I_h	I_d	H_O	T_{max}	T_{min}
17-Jan	22.3	10.2	41	27	17
16-Feb	21.5	9.8	39.6	26	17
16-Mar	21.3	8.4	36.5	27	16
15-Apr	20	6.1	31.8	26	13
15-May	16.6	4.3	27.3	24	11
11-Jun	17.2	3.6	25.1	22	9
17-Jul	18.4	3.9	26	21	8
16-Aug	21.1	4.1	29.7	24	10
15-Sep	23.9	5.6	34.6	27	13
15-Oct	24.9	7.1	38.4	28	15
14-Nov	23.5	8.1	40.5	28	16
10-Dec	21.8	10.2	41.2	27	17

Table 6.3 source of meteorological data from Jain P.C. (1984),

Tmax and Tmin form www.accuweather.com/en/zw/harare/353558

Predicted tank storage temperatures for Harare from January to December in degrees centigrade.

	jan	Feb	Mar	Apr	May	Jun	Jul	Aug	Sep	Oct	Nov	Dec
1	40	42	44	45	43	44	44	46	47	45	41	39
2	39	41	43	44	42	43	44	46	46	44	41	38
3	39	40	43	44	41	43	43	45	46	44	40	38
4	38	40	42	43	41	42	42	44	45	43	40	38
5	38	39	42	42	40	41	42	44	44	43	39	37
6	37	39	41	42	39	40	41	43	44	42	39	37
7	37	38	40	41	38	39	40	41	42	41	38	36
8	39	39	39	39	39	39	39	39	39	39	39	39
9	39	39	39	39	39	39	39	39	39	39	39	39
10	38	39	40	40	39	40	40	40	40	39	38	38
11	40	41	43	43	42	43	43	44	44	43	41	40
12	44	45	47	48	47	48	49	50	50	48	45	43
13	48	50	53	54	52	54	55	56	57	54	50	47
14	52	54	58	60	57	60	61	62	63	59	54	51
15	55	57	61	64	60	64	65	67	67	63	57	54
16	56	59	63	65	62	65	67	69	69	65	59	55
17	54	57	62	64	61	64	65	68	68	63	57	53
18	52	54	59	61	58	61	62	64	64	60	54	50
19	49	52	56	57	54	57	58	60	61	57	51	48
20	47	49	53	54	51	54	54	57	57	54	49	46
21	45	46	50	51	48	50	51	53	54	51	46	43
22	43	45	48	49	46	48	49	51	51	49	44	42
23	41	43	46	47	44	46	47	49	49	47	43	40

24	41	42	45	46	43	45	45	47	48	46	42	40

Table 6.4

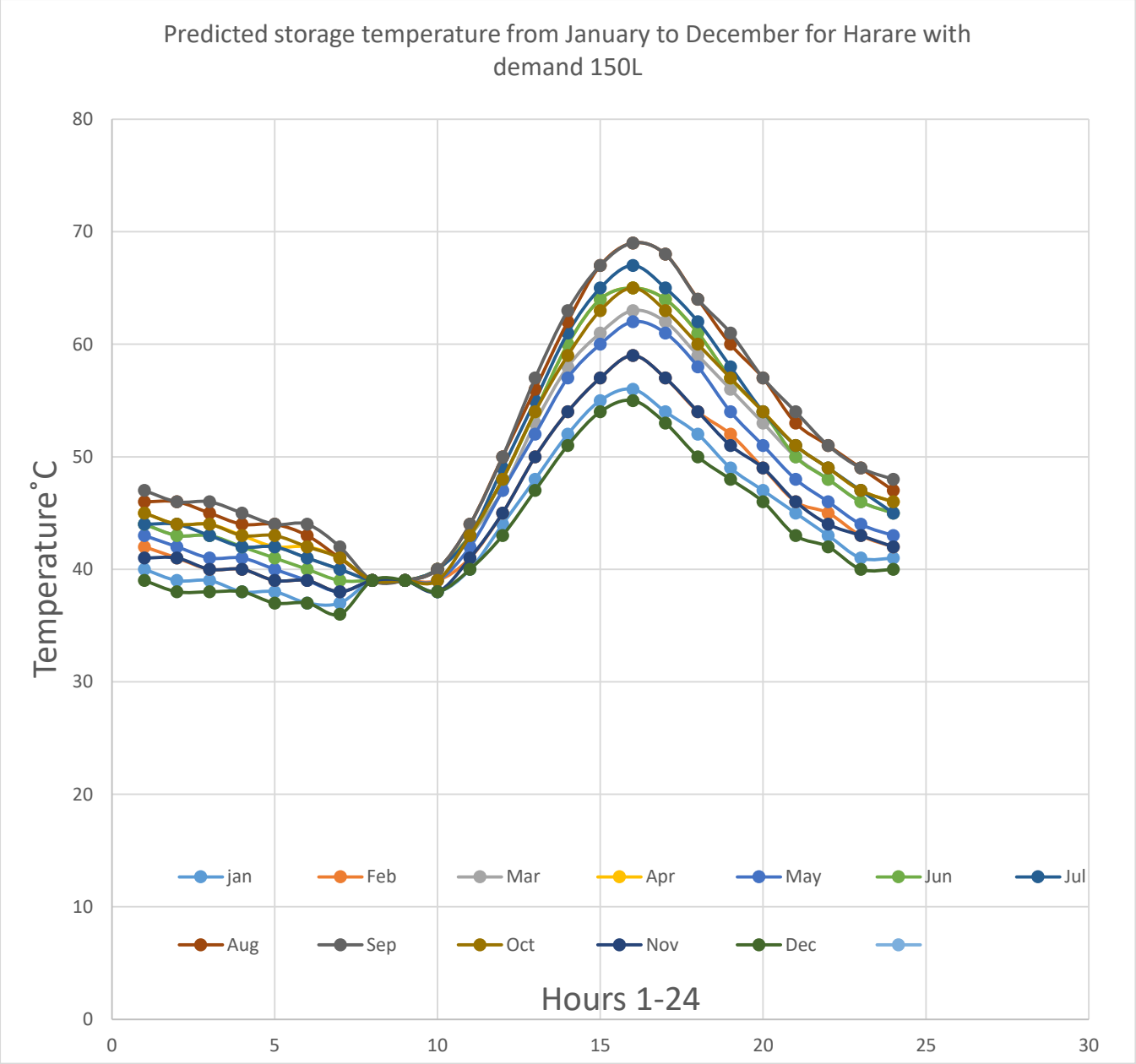

Fig.6.3

The kink in the graph at around 8:00 am is the time the experiment was began and in the graph this hour and temperature is recorded and initialised.

Table 6.5

Collector output throughout the year compared to the incident irradiation.

	Total incident irradiation/m^2 (kWh/day m^2)	Collector output energy/m^2 (kWh/day m^2)
Jan	5	1.98
Feb	5.2	2.25
Mar	5.7	2.66
Apr	6.1	2.92
May	5.6	2.65
Jun	6.3	3
Jul	6.7	3.14
Aug	6.9	3.29
Sep	6.7	3.22
Oct	6.1	2.8
Nov	5.3	2.2
Dec	4.8	1.83

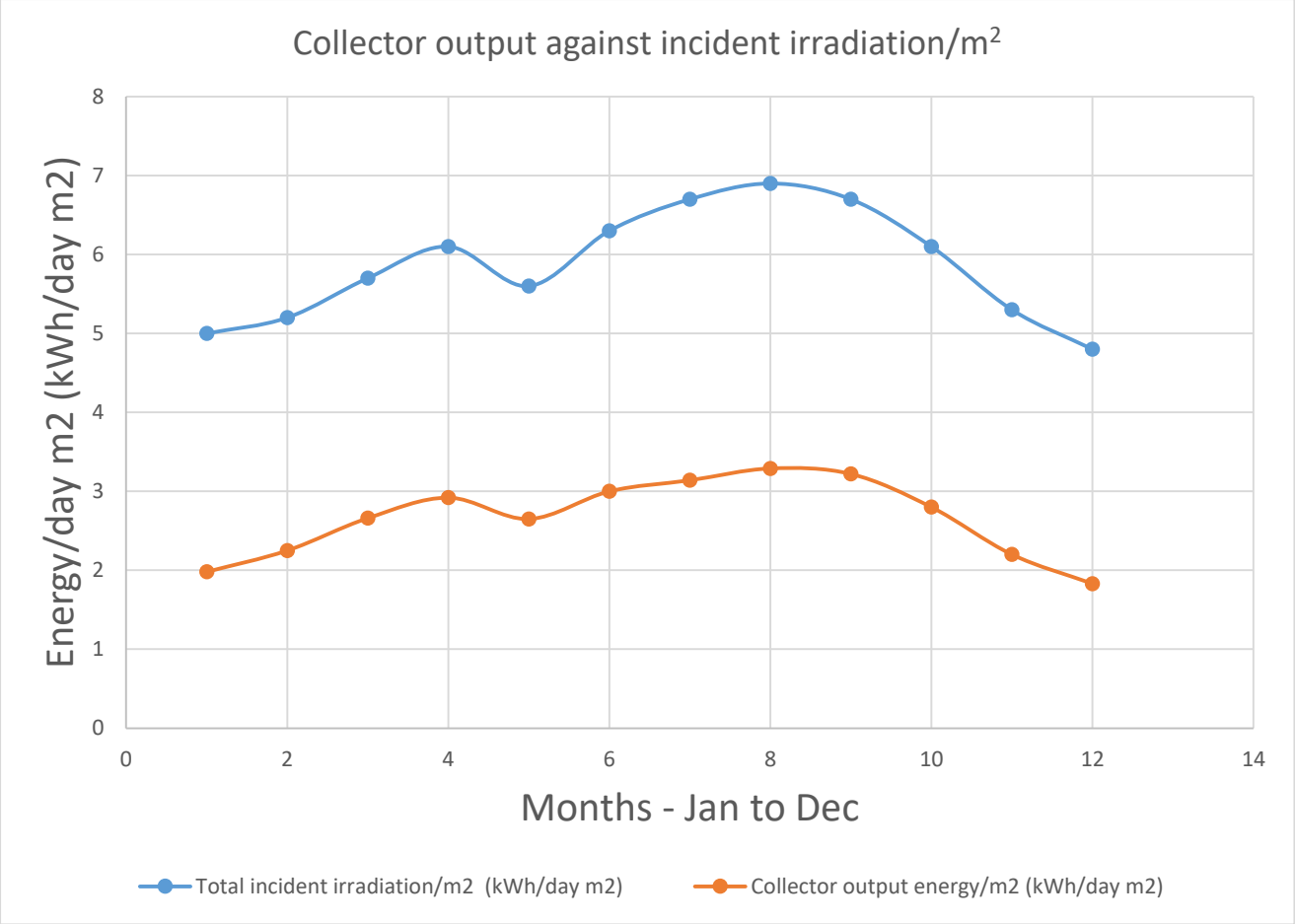

Fig.6.4

Collector output against incident radiation.

Table 6.6

	Daily collector efficiency %
Jan	40
Feb	43
Mar	47
Apr	48
May	47
Jun	48
Jul	47
Aug	48
Sep	48
Oct	46
Nov	42
Dec	38

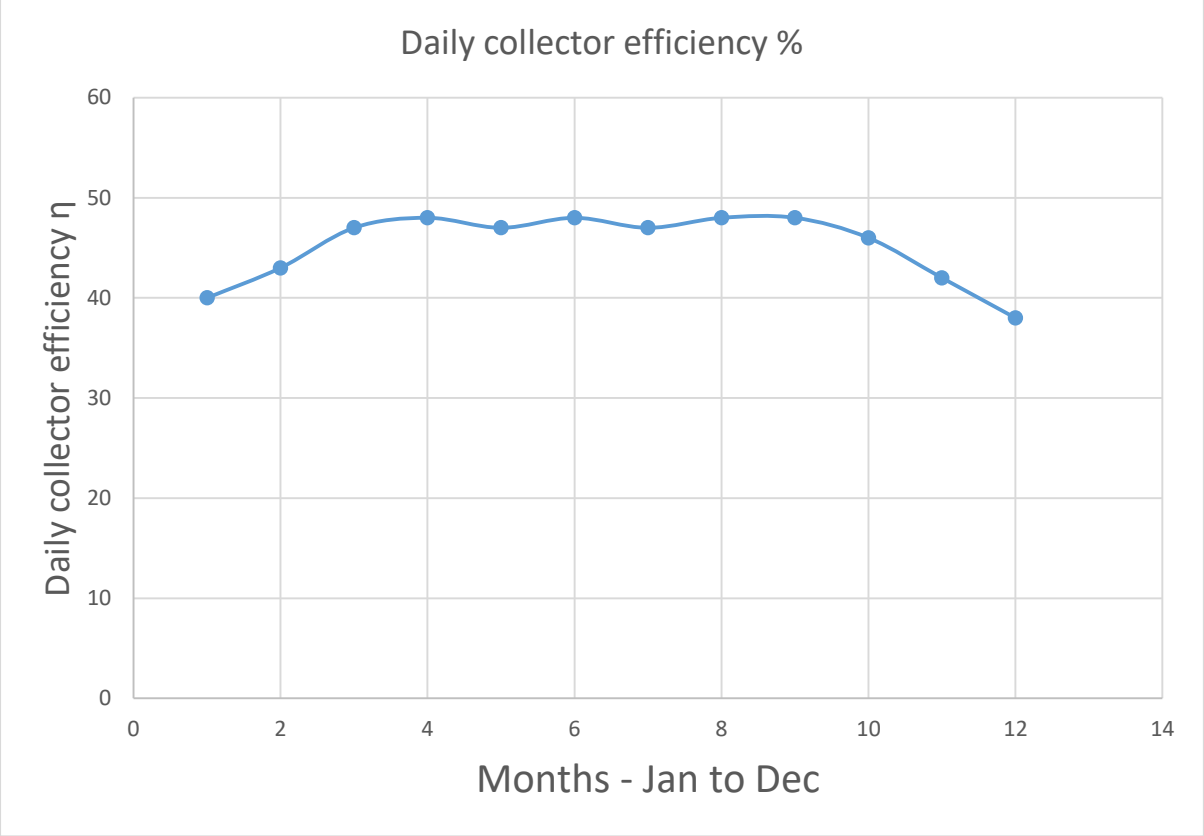
Daily collector efficiency %
Daily collector efficiency η
60
50
40
30
20
10
0
0
2
4
6
8
10
12
14
Months - Jan to Dec

Fig.6.5

	Average daily solar fraction
Jan	0.8
Feb	0.83
Mar	0.87
Apr	0.88
May	0.86
Jun	0.88
Jul	0.89
Aug	0.9
Sep	0.9
Oct	0.87
Nov	0.82
Dec	0.78

Table 6.7

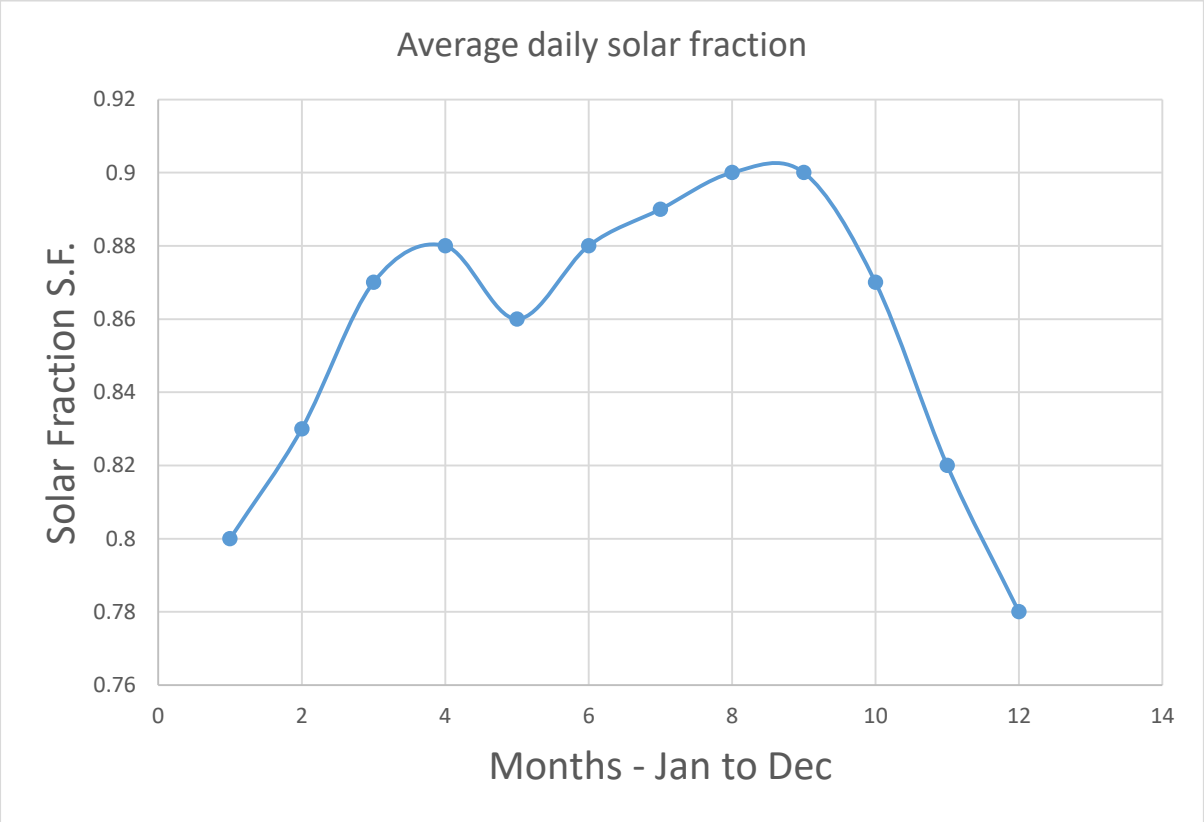

Analysis of collector performance by month

Month by month analysis of results show that December performs the worst from solar energy output of the collector, solar fraction and daily collector efficiency. This is because in Zimbabwe December is the wettest month and the sky is characterised by clouds albedo. August and September are the most efficient months in terms energy conversion by the solar collector and in terms of solar fraction.

CHAPTER 7

Economic analysis.

The following economic factors were used:

Collector warranty:	10 years
Cost per area	$220
Cost per volume	$2000
Installation % of total	35%
Inflation	1%
Interest rate	13%
O & M costs	2%
Electricity costs	0.11

GHG emission factors

CO_2 emission factor	0.91
Fossil fraction	0.6

The excel based computing model by Engineer Hove was used to evaluate economic parameters.

Results

Economic Outputs

Collector capital cost	$515
storage capital costs	$300
Total capital cost	$1 100
Specific investment	$7333/$m^3$
Annual Maintenance cost	$22
Net Present Value	$859
Specific Net Present Value	$5728/$m^3$
Internal Rate of Return IRR	25%
Annual Energy by Solar	2.8MWh/yr
Greenhouse gas averted	1.54 tonnes/yr

Table 7.1

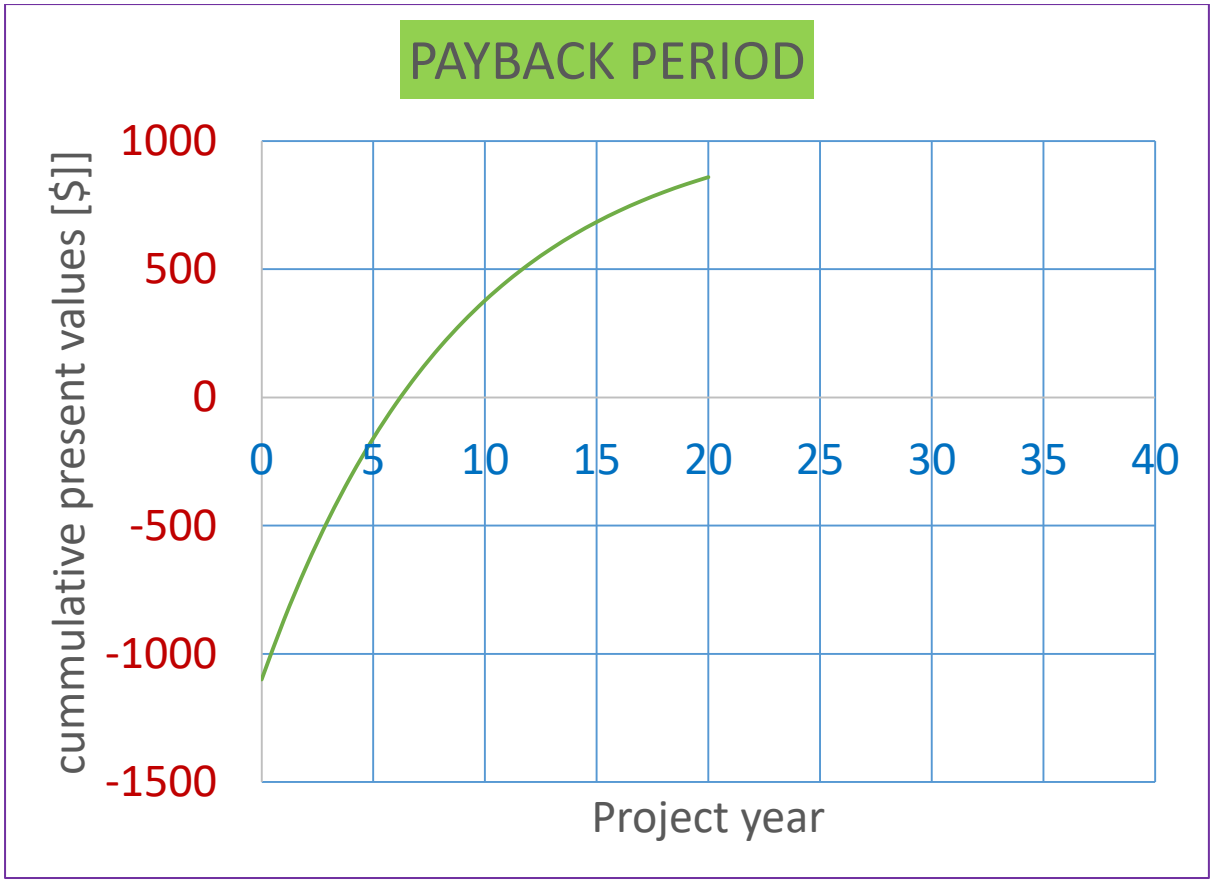

Fig.7.1

Payback period is after 7 years.

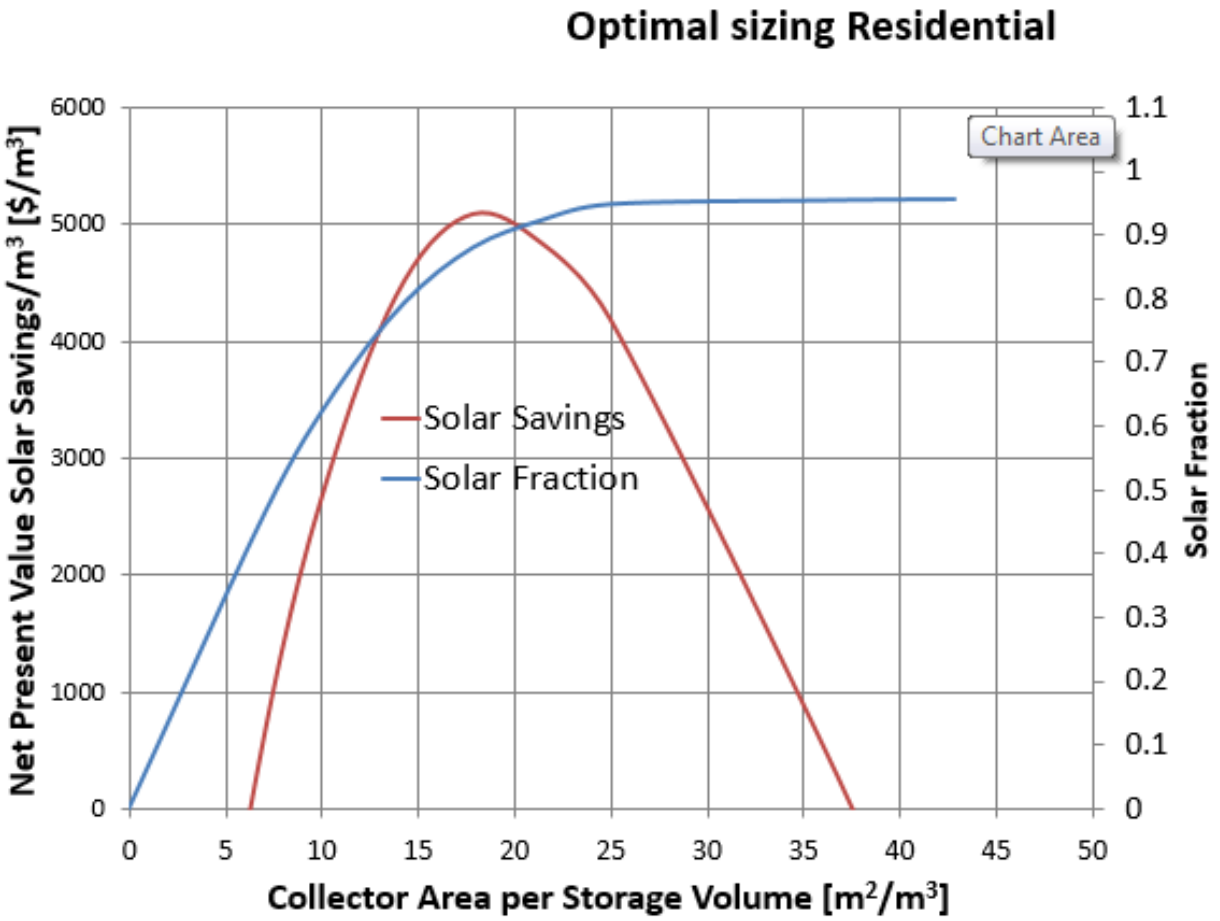
Optimal sizing Residential
Chart Area
Net Present Value Solar Savings/m³ [$/m³]
Solar Fraction
Collector Area per Storage Volume [m²/m³]
Solar Savings
Solar Fraction
6000
5000
4000
3000
2000
1000
0
1.1
1
0.9
0.8
0.7
0.6
0.5
0.4
0.3
0.2
0.1
0
0
5
10
15
20
25
30
35
40
45
50

Fig.7.2

CHAPTER 8

Conclusion and Recommendations

The main conclusion of this study is that this simple and inexpensive method of evaluating the optical and thermal parameters of SWH systems gives credible results.

Improvements to the method is the use of a data logger to insure simultaneous readings are captured for the various parameters that need readings taken at the same time.

A pyranometer at the tilted collector needs to be installed to ensure direct reading of radiation on a tilted plane rather modelled ones.

The solar collector panel frame needs to be reengineered to ensure that it can be set to optimise the radiation captured by the collector.

More experiments must be conducted in different periods of the year to get the overall behaviour of the system under different conditions.

As more experiments are performed there will be refinements and improvements such that the method can be adopted as a credible way of certification of SWH systems.

Bibliography

Duffie, J.A. and W.A, Beckman *Solar Engineering of Thermal Processes,* 4th Edition, 2013 (Wiley and Sons)

Kagande, L et al "Assesment of the economic impact of full scale use of domestic solar water heaters in Zimbabwe in comparison with other electrical management options," *International Journal of Science and Research (IJSR) Vol 2, Issue 1, January 2013* pp 363 – 382

Hove, T. and Gottsche, J. *Mapping global, diffuse and beam solar radiation over Zimbabwe*, 1999

Liu, B.H.Y. Jordan, R.C. *Daily insolation on surfaces tilted towards the equator*, Trans ASHRAE 1962

Orgill, J.F. and Hollands. K.G.T. *Correlation equation for hourly diffuse radiation on horizontal surfaces*, 1977

Kalogirou, S.A. *Solar Water Heating Systems,* 2009 (Elsevier)

Kalogirou, S.A Solar Collector Performance, 2009 (Elsevier)

SRCC, *Directory of SRCC certified solar collector rating,* 2006

Sruckman, F. *Analysis of a Flat Plat Collector*, 2008

Government of Zimbabwe publications, Ministry of Energy, National Energy Policy, 2012

Kok Seng Ong et al, *Reverse flow in natural convection heat pipe solar water heater*, 2014

IEA, *The characterisation and testing of solar collector thermal performance*,1993

Meyer J.P. *A review of domestic hot water consumption in South Africa,* 2000 ResearchGate

Burch J. and Magnuson L. *Diagnosis of Solar water heaters using solar storage tank surface temperature data*, 2009 (National Renewable Energy Laboratory)

Jain P.C. international Centre for theoretical Physics, Trieste 1984

Davidson J.H. et al, *A coefficient to characterise Mixing solar water Storage Tanks, Vol 116 May, 1994* (ASME Journal of Solar Energy Engineering)

Hamidi S.T et al, *Prediction of thermal characteristics for Solar Water Heater*, 2011

Kotak Y. et al, *Investigating the impact of ground albedo on performance of PV systems*, 2015 (CIBSE Technical Symposium)

https://en.wikipedia.org/wiki/Sunlight#/media/File:Solar_spectrum_en.svg

https://elfindingpolaris.wordpress.com/the science-of-stars/

www.e.education.psu.edu/

www.accuweather.com/en/zw/harare/353558